

# Recent Advances in Image Dehazing

Wencheng Wang, *Member, IEEE*, and Xiaohui Yuan, *Member, IEEE*

**Abstract**—Images captured in hazy or foggy weather conditions can be seriously degraded by scattering of atmospheric particles, which reduces the contrast, changes the color, and makes the object features difficult to identify by human vision and by some outdoor computer vision systems. Therefore image dehazing is an important issue and has been widely researched in the field of computer vision. The role of image dehazing is to remove the influence of weather factors in order to improve the visual effects of the image and provide benefit to post-processing. This paper reviews the main techniques of image dehazing that have been developed over the past decade. Firstly, we innovatively divide a number of approaches into three categories: image enhancement based methods, image fusion based methods and image restoration based methods. All methods are analyzed and corresponding sub-categories are introduced according to principles and characteristics. Various quality evaluation methods are then described, sorted and discussed in detail. Finally, research progress is summarized and future research directions are suggested.

**Index Terms**—Atmospheric scattering model, image dehazing, image enhancement, quality assessment.

## I. INTRODUCTION

UNDER bad weather conditions, such as fog and haze, the quality of images degrades severely due to the influence of particles in the atmosphere. Suspended particles will scatter light and result in attenuation of reflected light from the scene and the scattered atmospheric light will also mix with the light received by the camera and change the image contrast and color. Fig. 1 shows a comparison between a haze-free image and a hazy image. It can be seen from Fig. 1 (a) that the scattered light due to the haze greatly reduces the image contrast, and the image color appears dull compared to Fig. 1 (b).

Therefore, it is necessary for computer vision systems to improve the visual effects of the image and highlight image features. Image dehazing technique, also known as “haze removal” or “defogging” is just the technique to reduce or

Manuscript received February 5, 2016; accepted January 16, 2017. This work was supported by the National Natural Science Foundation of China (61403283), Shandong Provincial Natural Science Foundation (ZR2013FQ036, ZR2015PE025), the Spark Program of China (2013GA740053), the Spark Program of Shandong Province (2013XH06034), and the Technology Development Plan of Weifang City (201301015). Recommended by Associate Editor Jvfu Feng. (*Corresponding author: Wencheng Wang*)

Citation: W. C. Wang and X. H. Yuan, “Recent advances in image dehazing,” *IEEE/CAA J. of Autom. Sinica*, vol. 4, no. 3, pp. 410–436, Jul. 2017.

W. C. Wang is with the College of Information and Control Engineering, Weifang University, Weifang 261061, China (e-mail: wwwcfu@126.com).

X. H. Yuan is with the Department of Computer Science and Engineering, University of North Texas, Denton 76207, TX, USA (e-mail: xiaohui.yuan@unt.edu).

Color versions of one or more of the figures in this paper are available online at <http://ieeexplore.ieee.org>.

Digital Object Identifier 10.1109/JAS.2017.7510532

even remove interference due to haze by special approaches, in order to obtain satisfactory visual effects and obtain more useful information. In theory, image dehazing removes unwanted visual effects and is often considered as an image enhancement technique. However, it differs from traditional noise removal and contrast enhancement methods since the degradation to image pixels that is induced by the presence of haze depends on the distance between the object and the acquisition device and the regional density of the haze. The effect of haze on image pixels also suppresses the dynamic range of the colors.

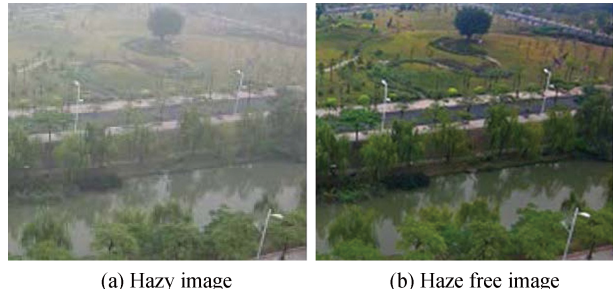


Fig. 1. Comparison between hazy image and haze free image.

The development of image dehazing methods has been beneficial to many real-world applications, including video assisted transportation [1]–[4], outdoor video surveillance [5]–[10], analysis of remote sensing imagery [11]–[17], and driver assistance systems [18]–[27]. These techniques can also be transferred to underwater image enhancement [28]–[33] and images acquired in rain or snow [34]–[39]. Bissonnette made early efforts to improve the quality of images acquired in foggy and rainy conditions [40]. The broad prospects for applicability have attracted much attention from researchers and it has become a research hotspot in computer vision and image processing fields in recent years. According to statistics on literature in English, the number of papers on this subject has increased every year. Fig. 2 displays the number of related papers in English searched by Google Scholar from 2000 to 2014 (blue solid line) and the number of papers published by famous international conferences (red dotted line).

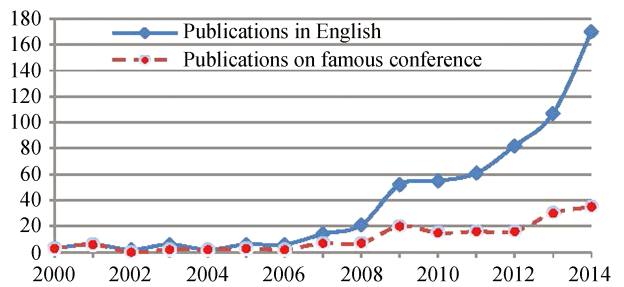


Fig. 2. Quantity of papers published in recent years.

Although a large number of image dehazing methods have been proposed, the research is still scattered and a complete theoretical system has still not been established. In particular, there is a lack of systematic summary of the advances in related work until now [41]. Therefore, it is necessary to summarize the development of image dehazing methods in the last decade. This paper provides an extensive review of the recent advances of image dehazing techniques and related methods. To facilitate a comprehensive overview, existing techniques are categorized based on their principles and characteristics. In addition, various quality evaluation methods are described and discussed in detail, and research progress is summarized and future research directions are suggested. In this paper, we try to elaborate on existing image dehazing methods including application characteristics, dehazing performance, algorithm complexity and other aspects.

The remainder of this paper is organized as follows. Section II introduces the dehazing methods according to their classification in Fig. 3 and their principles and characteristics are analyzed in detail. In Section III, related quality assessment criteria of dehazing algorithms are described. Finally, a summary of conclusions is given and future research directions are suggested in Section IV.

## II. CLASSIFICATION OF DEHAZING ALGORITHMS

Based on differences in dehazing principles, current methods can be divided into three categories: image enhancement based methods, image fusion based methods and image restoration based methods. Image enhancement based methods do not take the cause of the image degradation into account, but mainly use targeted image processing methods to improve the contrast and details, and improve the visual effects of the image. Image fusion based methods maximize the beneficial information from multiple source channels to finally form a high quality image, without requiring a physical model. Image restoration based methods establish a foggy image degradation model by studying the physical mechanisms of optical imaging, invert the degradation processes and compensate for distortion caused by these degradation processes in order to obtain clear images without haze. Each of the above three categories can also be sub-divided into different subclasses, and some of these algorithms can be extended for video dehazing. All of the main categories are described in Fig. 3.

### A. Image Enhancement Methods

Image enhancement based methods are not required to solve the physical model of image degradation, but rather directly enhance the image contrast and improve the image quality from the perspective of human visual perception. These methods mainly include histogram equalization, the Retinex method and frequency domain enhancement.

#### 1) Histogram Equalization

Histogram equalization is a basic algorithm for low contrast images. In a hazy image, the layer of “haze” will result in a narrow range of grayscales, and the contrast is decreased. Through histogram equalization processing, the entire range of gray values are distributed uniformly across a higher dynamic

range, to improve the image contrast and enhance the details of the image. In other words, histogram equalization enhances the overall contrast of a hazy image by increasing the dynamic range of the gray values. An example is shown in Fig. 4: (a) is a hazy image, (b) is the histogram of (a), (c) is the dehazed image from (a), and (d) is the histogram of (c).

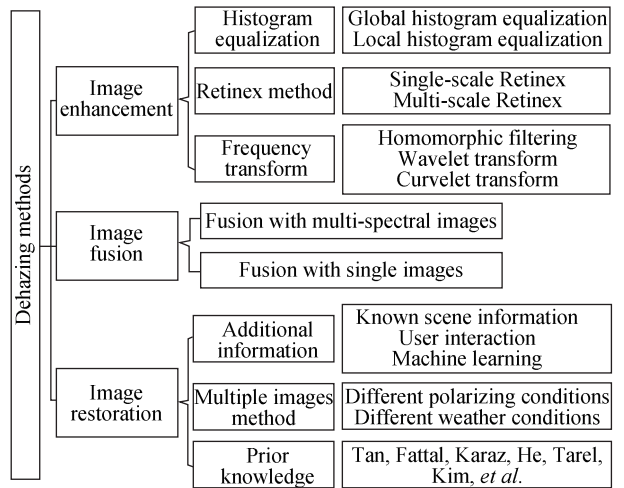


Fig. 3. Classification of image dehazing methods.

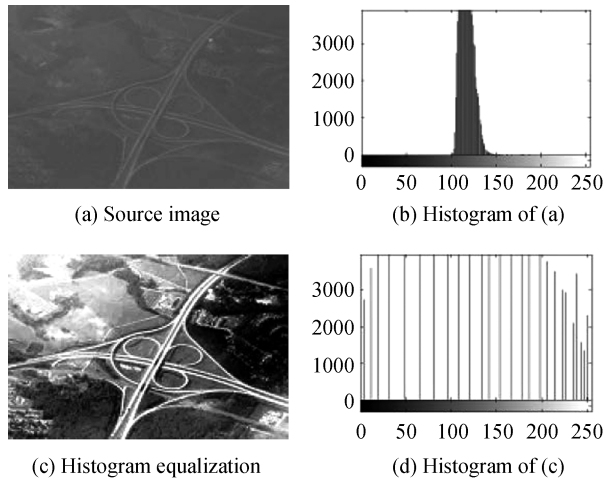


Fig. 4. Dehazing with histogram equalization.

Depending on the difference in the computing region, histogram equalization can be divided into global histogram equalization (GHE) and local histogram equalization (LHE).

GHE uses the cumulative distribution function as the transformation curve of the gray values. Suppose variables  $r$  and  $s$  are the grayscales of the original image and the processed image, respectively;  $P_r(r)$  is the probability of  $r$ ;  $L$  is the maximum grayscale value;  $n$  is the sum of the pixels in the image;  $n_j$  is the number of the  $j$ th grayscale. Then, the histogram equalization can be expressed as:

$$s = T(r) = \sum_{j=0}^k P_r(r_j) = \sum_{j=0}^k \frac{n_j}{n}, \quad k = 0, 1, 2, \dots, L-1. \quad (1)$$

The advantage of GHE is that it has lesser computations with a high efficiency and is particularly suitable for the

enhancement of images that are too dark or bright overall. It is usually used to compress the brightness of pixels to obtain more uniform exposure characteristics [42]. However, the algorithm's gray statistics across the whole image make it difficult for each local area to restore the optimal values since the method cannot adapt to the local brightness characteristics of an input image, and often causes a "halo" effect and brightness distortion. Therefore, some scholars have proposed a local histogram equalization algorithm to solve this problem which has been widely used.

LHE extends the histogram equalization algorithm to all local regions of the image, and adaptively enhances local information of the image by local operations. It is suitable for processing a hazy image with low contrast and a changeable depth of field, but block effect usually appears and the calculation complexity is large. Local histogram equalization methods have been proven to provide better performance than global methods and reveal more local image details with stronger image enhancement performance [43]–[45].

Some optimized methods will now be described. Reference [46] used adaptive histogram equalizations (AHE) for contrast enhancement while [47] used partially overlapped sub-block histograms to enhance the contrast. Huang *et al.* [48] have proposed a novel local histogram equalization algorithm which had good performance for improving the contrast of the image while preserving the brightness. Xu *et al.* [49] have established a generalized equalization model that integrates contrast enhancement and white balancing into a unified framework for convex programming of the image histogram. In [50], histogram equalization and a wavelet transform (WT) method are combined to enhance images, which can improve the gray distribution of images. Xu *et al.* [51] have proposed a contrast limited adaptive histogram equalization (CLAHE) method to remove the effects of fog, which can limit noise while enhancing the image contrast. In [52] combined the CLAHE method with the Weiner filter and [53] combined the CLAHE method with the finite impulse response filter to enhance the contrast of images.

In summary, the histogram equalization algorithm can achieve better performance for gray images than for color images, and can lead to noise amplification in some hazy images.

## 2) Retinex Method

Retinex, i.e., retinal cerebral cortex theory, was created by Land and McCann based on color perception by the human eyes [54], [55]. Retinex-based algorithms have been widely applied in the field of image enhancement for applications such as shadow removal and haze removal. Its principal concept is to obtain the reflection properties of objects from the influence of light on the image, and it provides a model for describing the color invariance. The concept is based on the fact that during visual information transmission, the human vision system performs some information processing to remove the uncertainty related to the light source's intensity and irradiation, and only information reflecting the nature of the object, such as the reflection coefficient. The model of illumination reflection is shown in Fig. 5 and (2), which show that an image can be expressed as a reflection component and

an illumination component.

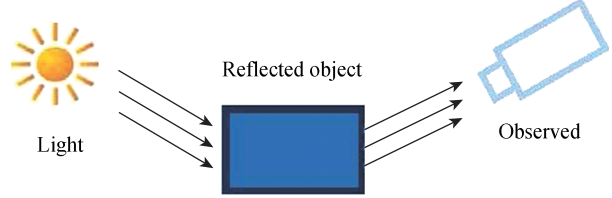


Fig. 5. The model of illumination reflection.

$$F(x, y) = R(x, y)I(x, y) \quad (2)$$

where  $R(x, y)$  is the reflection component, which represents the reflection of the surface of an object and is related to the intrinsic nature of the image,  $I(x, y)$  is the illumination component, which depends on the ambient light and is related to the dynamic range of the image and  $F(x, y)$  is the captured image. Based on Retinex theory, if a method can be found to estimate and separate the reflection component from the total light, the impact of the illumination component on the image can be reduced, achieving the goal of enhancing the image. The Retinex algorithm has the characteristics of color constancy, dynamic range compression and color fidelity, and its workflow is shown in Fig. 6, where  $\log$  is a logarithmic operation and  $\exp$  is an exponential operation.

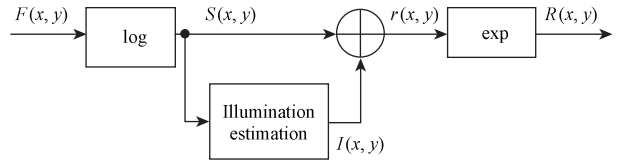


Fig. 6. Workflow of the Retinex method.

The Retinex method used for enhancement of hazy images can be divided into two categories: single-scale Retinex (SSR) and multi-scale Retinex (MSR).

An SSR algorithm has been proposed by Jobson *et al.* [56] based on the center/surrounding Retinex method. The essence of this algorithm is to obtain the reflection image by estimating the ambient brightness. In order to keep a good balance between the dynamic range compression and the color constancy, Rahman *et al.* [57] extended the SSR algorithm to multiple scales and proposed an MSR algorithm.

Since the reflection image has little dependence on the intensity of the illumination, the Retinex algorithm can easily realize image dehazing. The formulas for SSR and MSR can be expressed by (3) and (4), respectively.

$$\begin{aligned} r_i(x, y) &= \log R_i(x, y) \\ &= \log F_i(x, y) - \log[G(x, y) * F_i(x, y)] \end{aligned} \quad (3)$$

$$\begin{aligned} r_{MSR_i}(x, y) &= \log R_i(x, y) \\ &= \sum_{k=1}^N w_k \{\log F_i(x, y) - \log[G_k(x, y) * F_i(x, y)]\} \end{aligned} \quad (4)$$

where  $F(x, y)$  is the input image,  $r_i(x, y)$  is the output of the Retinex,  $R(x, y)$  is the reflection image,  $i$  is the color

channel,  $(x, y)$  is the position of a single pixel,  $*$  represents the convolution operator,  $N$  is the number of scales,  $G(x, y) = e^{-(x^2+y^2)/c^2}$  is the low-pass convolution surrounding function,  $w_k$  is the weighted coefficient, and  $c$  is the Gauss surrounding scale.

The algorithm combines the advantages of different Gaussian functions convolved with the original image, including the characteristics of large, medium and small scales, and can achieve high dynamic range compression and color constancy for better visual effects.

However, since Gaussian filtering does not have good edge preservation performance, the phenomena of edge degradation and “halo” artifacts will appear in the dehazing result. In order to solve these problems as much as possible, Xu *et al.* [58] estimated the illumination values by using a mean shift smoothing filter to overcome the uneven illumination and eliminate the halo phenomenon. Yang *et al.* [59] presented an adaptive filter which combined sub-block local information to estimate the luminance component. Hu *et al.* [60] used bilateral filtering to replace Gaussian filtering to estimate the illumination component. In [61], a novel Multi-Scale Retinex color image enhancement method has been proposed to enhance the contrast and better preserve the color of the original image. In this method, the orientation of the long axis of the Gaussian filter is determined according to the gradient orientation at that position. Shu *et al.* [62] also proposed a type of MSR algorithm based on sub-band decomposition for image enhancement. Fu *et al.* [33] proposed a variation framework for Retinex to process the reflection and the illumination from a single underwater image by decomposing, enhancing and combining after color correction. Zhang *et al.* [63] adopted an improved Retinex-based method to remove fog in a traffic video. Experimental results showed that the proposed method can not only remove the fog but also enhance the clarity of the traffic video images.

The advantages of the Retinex algorithm are clear and easy to implement. These methods can not only increase the contrast and brightness of the image, but also can regulate the dynamic range of the gray level with a priority given to color image dehazing. However, the algorithm uses the Gaussian convolution template for illumination estimation and does not have the ability to preserve edges, which will lead to halo phenomena in some sharp boundary regions or cause the whole image to be too bright.

### 3) Frequency Domain Filtering

Under foggy conditions, the low frequency components of an image are enhanced, so a high-pass filter can be used for image filtering to suppress low frequencies and enhance high frequencies. The frequency domain enhancement always uses Fourier analysis and other methods to convert an image into the frequency domain. After completing the filtering operation, an inverse transform is performed back to the spatial domain. Typical methods based on the frequency domain include homomorphic filtering, the wavelet transform and the Curvelet transform.

a) The principle of homomorphic filtering is to divide the image into a radiation component and a reflection component. The radiation component of the foggy image is characterized

by a slow variation in space, and the reflection component is often associated with the details of the scene. Image enhancement is achieved by removing the radiation component. By combining frequency filtering with the gray scale transformation, the dynamic range of the compressed image can be used to improve the image quality.

Thus, the basic principle of homomorphic filtering for dehazing is still based on the illumination model. The flowchart of this algorithm is shown in Fig. 7, where log is the logarithmic transform, FFT is the Fourier transform,  $H(u, v)$  is the frequency filtering function, IFFT is the inverse Fourier transform and exp is the exponential operation.

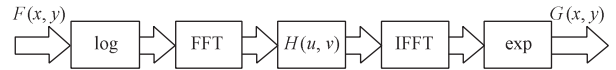


Fig. 7. The flowchart of homomorphic filtering.

Seow *et al.* [64] processed foggy color images using a homomorphic filter and achieved good enhancement effects. In [65], a self-adaptive homomorphic filtering method is proposed to remove thin clouds.

The homomorphic filtering algorithm can remove uneven regions generated by light, while maintaining the contour information of the image. However, it needs two Fourier transformations, one exponential operation and one logarithmic operation for each pixel of the image, so the computation is large.

b) The basic principle of the wavelet transform (WT) is similar to homomorphic filtering for image enhancement. Firstly, a wavelet transform is performed on the original image, and images with different frequency characteristics are obtained. The details of the image are then enhanced for the non-low frequency sub blocks to improve their clearness.

The WT can be described by the following steps: perform displacement processing on the basic wavelet function  $\psi(t)$  at step  $\tau$ , then create a product with signal  $x(t)$  for different scales  $a$ :

$$WT_x(a, \tau) = \frac{1}{\sqrt{a}} \int_{-\infty}^{+\infty} x(t) \psi^* \left( \frac{t - \tau}{a} \right) dt, \quad a > 0. \quad (5)$$

Its equivalent expression in the frequency domain is:

$$WT_x(a, \tau) = \frac{\sqrt{a}}{2\pi} \int_{-\infty}^{+\infty} X(\omega) \Psi^*(a\omega) e^{j\omega\tau} d\omega \quad (6)$$

where  $X(\omega)$  and  $\Psi(\omega)$  are the Fourier transform of  $x(t)$  and  $\psi(t)$ , respectively.

Gewe *et al.* [66] proposed a fusion method based on wavelet analysis, and fused and processed a large number of foggy images to obtain a high quality visual effect. Russo [67] implemented equalization with different scales on a degraded image, and achieved good sharpening results of the details. Du *et al.* [68] suggested that haze is distributed in the low-frequency layer, and thus introduced a single-scene based haze masking method that uses wavelet analysis to decompose a hazy image. However, the application of this method is limited to ice/snow-free scenes. Reference [69] assumed that the fog is mainly in low frequency regions while scene details are in high frequency regions, and improved the image quality by

dehazing the low frequency regions and enhancing the high frequency regions. Zhu *et al.* [70] applied the wavelet transform to image dehazing, and then used the SSR algorithm to enhance the color performance and get the expected haze-free image. Reference [71] described a new method for mitigating the effects of atmospheric distortion using a regional fusion method based on the dual tree complex wavelet transform (DT-CWT) which improved the visibility. John *et al.* [72] introduced a wavelet based method for enhancing weather degraded video sequences, which processed the foreground and background pixels of the reduced quality video using wavelet fusion theory.

The WT is a local transformation of space and frequency and has advantages of multi-scale analysis and multi-resolution characteristics for image contrast enhancement. However, over-bright, over-dark and unevenly illuminated images are difficult to resolve.

c) The curvelet transform (CT) is a multi-scale analysis method developed from the wavelet transform, which can overcome the edge enhancement limitation of WT. CT has been used to perform automatic processing of foggy images. Starck *et al.* [73] presented a new method for contrast enhancement based on the CT, which can represent edges better than wavelets, and is therefore well-suited to multi-scale edge enhancement. The authors also found that curvelet based enhancement out-performs other enhancement methods for noisy images, but on noiseless or near noiseless images, curvelet based enhancement is not much effective than wavelet based enhancement. In [74], the authors implemented an efficient algorithm which can extract a clear image from a blurred and hazy image by using the curvelet to increase the clarity of the image as well as removing image haze.

Although it can improve the visual image quality by enhancing the curved edges, it cannot in essence remove interference due to fog from the image. Its general application includes SAR (synthetic aperture radar) image enhancement and ceramic micro image enhancement.

In summary, the main purpose of foggy image enhancement is to satisfy the visual effect requirement for the human eyes, or make computer recognition easier. While the image quality is not considered, the methods only need to highlight certain information while reducing or removing the information that is unnecessary within an image. Since there is no physical mechanism and degradation model for foggy image processing, this is not essentially dehazing, especially for foggy color images, which generally cannot achieve a satisfactory result.

## B. Image Fusion Based Methods

Image fusion is the process of combining relevant information from multiple source channels into a high quality image. Fusion strategies should maximize the extraction of information from each channel in order to improve the utilization of image information. These methods have also been used in image dehazing in recent years. The details of these methods are given as follows.

### 1) Fusion With Multi-spectral Images

Near-infrared (NIR) light has stronger penetration capability than visible light due to its long wavelengths, and is thus

less scattered by particles in the air. This makes it desirable for image dehazing to reveal details of distant objects in landscape photographs. The near-infrared spectrum can easily be acquired by using off-the-shelf digital cameras with minor modifications [75], or potentially through a single RGBN camera which can capture multiple images with different properties simultaneously.

Schaul *et al.* [76] took advantage of the fact that NIR images are less sensitive to haze and proposed a method to dehaze images using both visible and NIR images. In their method, the optimization framework of the edge preserving multiresolution decomposition is applied to both the visible and the NIR images based on weighted least squares (WLS), and a pixel level fusion criterion is used to maximize the image contrast. The advantage of this approach for dehazing is that there is no requirement for a scattering model. An example is shown in Fig. 8. In contrast with [76], reference [77] performed dehazing on visible images and infrared images by firstly using a processing method, and then used a fusion strategy to complete the image fusion. In [78], the authors proposed a two-stage dehazing scheme: an air-light color estimation stage that exploits the dissimilarity between RGB and NIR; and an image dehazing stage that enforces the NIR gradient constraint through an optimization framework. This method also achieved good results.

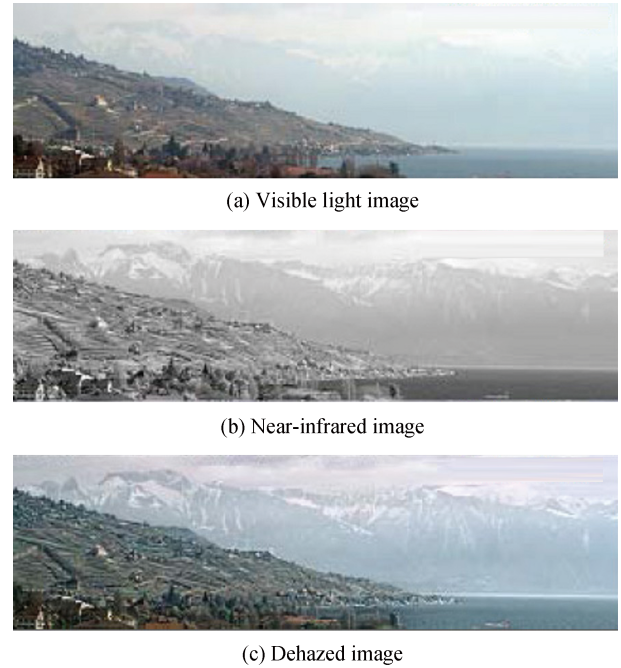


Fig. 8. Dehazing with multi-spectral images.

Since these methods do not need to detect the fog and atmospheric light, there is no depth map required. However, it is difficult to obtain the source images and several halo artifacts may be seen.

### 2) Fusion With a Single Image

Ancuti *et al.* [79]–[81] first demonstrated the utility and effectiveness of a fusion-based technique for dehazing a single degraded image. The two images for fusion are both derived from the original hazy image  $I(x)$ , and these inputs are

weighted by three normalized weight maps (luminance, chromatic, saliency) and finally blended in a multi-scale fashion that avoids introducing artifacts.

The first input  $I_1(x)$  is obtained by white-balancing the original hazy image. The second image  $I_2(x)$  is obtained by subtracting the original image from the mean image using the expression:

$$I_2(x) = \gamma (I(x) - \bar{I}(x)) \quad (7)$$

where  $\gamma$  is a factor that increases linearly with luminance in hazy regions.

In order to balance the contribution of each input and ensure that regions with high contrast are obtained, three measures (weight maps) are introduced: the luminance weight map  $W_L^k(x)$ , the chromatic weight map  $W_C^k(x)$  and the saliency weight map  $W_S^k(x)$ , where  $k$  is the index of the inputs.

Assume that the resulting weights  $W^k$  are obtained by multiplying the processed weight maps  $W_L^k$ ,  $W_C^k$  and  $W_S^k$ . Then, each pixel  $x$  of the output  $F$  is computed by summing the inputs  $I_k$  weighted by corresponding normalized weight maps  $W^k$ :

$$F(x) = \sum_k \bar{W}^k(x) I_k(x) \quad (8)$$

where  $I_k$  symbolizes the input ( $k$  is the index of the inputs) and  $\bar{W}^k = W^k / \sum_k W^k$  are the normalized weight maps.

Using Gaussian and Laplacian pyramids, the above equation becomes:

$$F_l(x) = \sum_k G_l\{\bar{W}^k(x)\} L_l\{I_k(x)\} \quad (9)$$

where  $l$  represents the number of pyramid levels and  $L\{\cdot\}$  and  $G\{\cdot\}$  are the Laplacian and Gaussian pyramids, respectively.

The final haze-free image  $J$  is obtained by summing the contribution of the resulting inputs (the levels of the pyramid):

$$J(x) = \sum_l F_l(x) \uparrow^d \quad (10)$$

where  $\uparrow^d$  is the upsampling operator with factor  $d = 2^{l-1}$ .

This technique is focused on restoring the latent image without estimating the atmospheric light and transmission (depth) map, and no post-processing steps are required to implement. Thus the method is computationally effective.

This method was later used for underwater enhancement [82], with some proposed improvements. For example, in [83], the first input image is obtained via a simple linear transformation and the second image is obtained based on guided image filtering from a foggy image. The final defogged result is obtained using simple white balance after image fusion. In [84], two coarse transmission maps using prior dark channels are fused during the haze removal stage. One is obtained based on a single-point pixel and the other is obtained using a patch. The proposed approach simultaneously dehazes the image and enhances its sharpness by individually treating each model component and its residual. In [85], the foggy image is processed using white balancing and contrast stretching in turn, and the fusion strategy is used for the haze density, salient features and exposure level to effectively obtain the haze-free image. Another fusion-based strategy has been

proposed to combine the initial recovered image with an image with sufficient details and color information. The combined image is more informative than any of the input images and should also appear “natural” [86].

These methods employ a fusion-based strategy for two images derived from the original image, and thus the images are perfectly aligned. However, this technique is limited to processing only color images.

### C. Image Restoration Based Methods

Image restoration based methods for dehazing are studied to explore the reasons for the image degradation and analyze the imaging mechanism, then recover the scene by an inverse transformation. In this method, the physical model of the degraded images is the basis, and many researchers have used the following general model for image restoration.

1) *Degradation Model*: As shown in Fig. 9,  $f(x)$  is the input image,  $h(x)$  is the degradation function,  $n(x)$  is the noise,  $g(x)$  is the degraded image,  $h'(x)$  is the restoration function and  $f'(x)$  is the restored image. The linear time invariant system can be generally expressed as:

$$g(x) = f(x) * h(x) + n(x). \quad (11)$$

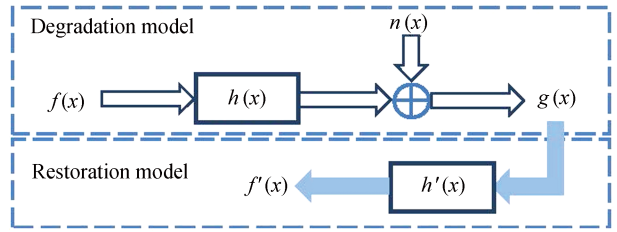


Fig. 9. Degradation and restoration model.

However, this model has some shortcomings: the model is simply expressed as a linear time invariant system, which ignores the physical process of image degradation and the degradation function and noise function in the model cannot easily and accurately express the complex factors of weather conditions. Therefore, the above model cannot achieve good results for foggy images.

2) *Physical Models Based on Atmospheric Scattering*: In 1998, Oakley *et al.* [87] started to use the Mie atmospheric scattering law to undertake some research work on images taken in bad weather conditions. The model-based dehazing method is now a research hotspot in the image processing field. In the last decade, some researchers have performed deep analysis of the degradation mechanism and foggy image modeling based on atmospheric scattering theory, and have made great progress and proposed some image processing methods to enhance image clearness.

According to atmospheric scattering theory, the scattering of atmospheric particles is mainly divided into two parts: one is due to the attenuation of reflected light from the object surface to the camera; and the other is the scattering of air-light reaching to the camera. Therefore, McCartney [88] proposed that the imaging mechanism in bad weather should be described by a light attenuation model and an air-light

imaging model, which forms a theoretical basis of a foggy image with characteristics of blur and low contrast that can be used to understand the degradation mechanism of foggy images, thus enabling degraded images to be restored. A schematic diagram of the atmospheric scattering model is shown in Fig. 10. The solid line is the light from the object to the camera, and the dotted line is the air-light.

The principle of the attenuation model is described in Fig. 11. If a beam of light is emitted into an atmospheric medium, when the incident light passes through a unit area (the shaded part), the energy of the light will then be attenuated. It can be expressed by (12).

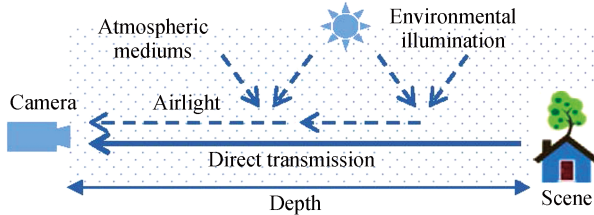


Fig. 10. Atmospheric scattering model.

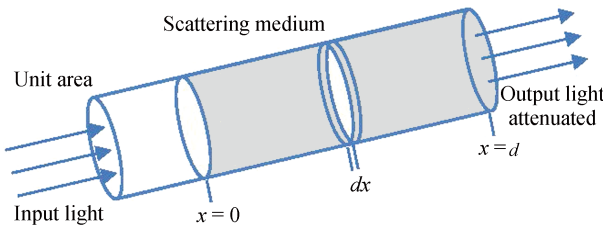


Fig. 11. Attenuation model.

$$E_d(d, \lambda) = E_0(\lambda)e^{-\beta(\lambda)d} \quad (12)$$

where  $\lambda$  is the wavelength of visible light,  $d$  is the distance from the scene to the camera,  $\beta(\lambda)$  is the atmospheric scattering coefficient and  $E_0(\lambda)$  is the beam radiation intensity at  $x = 0$ .

The principle of the airlight scattering model is described in Fig. 12. If it is assumed that the direction, intensity and spectrum of the atmospheric light are unknown, and that the light traveling along the line of sight has constant energy, then the radiation intensity reaching the camera can be expressed by (13).

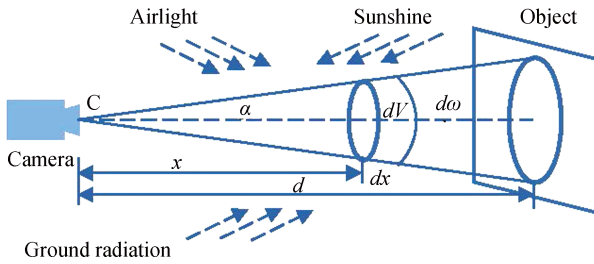


Fig. 12. Airlight scattering model.

$$E_a(d, \lambda) = E_\infty(\lambda)(1 - e^{-\beta(\lambda)d}) \quad (13)$$

where  $E_\infty(\lambda)$  is the radiation intensity of the atmospheric light at infinity.

According to the mechanisms of the McCartney model [88], the attenuation process and the airlight imaging process are both dominant and lead to a decrease in contrast of the foggy image. Therefore, the total radiant intensity received by the camera is equivalent to the linear superposition of the scene radiation light with the addition of scattered light entering the imaging system, and the formula is:

$$E(d, \lambda) = E_0(\lambda)e^{-\beta(\lambda)d} + E_\infty(\lambda)(1 - e^{-\beta(\lambda)d}) \quad (14)$$

where the first term is the direct attenuation, which describes the attenuated result of reflected light in the medium, and the second term is the airlight (the atmospheric veil), which reflects the scattering of global atmospheric light. Letting  $I(x) = E(d, \lambda)$  represent the hazy image,  $J(x) = E_0(\lambda)$  represent the haze-free image,  $t(x) = e^{-\beta(\lambda)d}$  denote the transmission, and  $A = E_\infty(\lambda)$  denote the atmospheric light (skylight or airlight color), then, equation (14) can be simplified to:

$$I(x) = J(x)t(x) + A(1 - t(x)). \quad (15)$$

As can be seen from (15), the main difficulties in solving single image dehazing are the double unknowns of the haze-free image  $J(x)$  and the transmission map  $t(x)$ , which are severely ill-posed. However, if the depth information of an image is known, or if multiple images can be used to estimate the depth, or some prior knowledge is available for a single image, the  $J(x)$  can still be resolved.

Therefore, in recent years, many scholars have used (14) or (15) as the prototype to propose a large number of dehazing algorithms, many of which have achieved satisfactory results. Several representative methods based on a physical model will now be introduced in the following section.

### 1) Single Image Dehazing With Additional Information

#### a) Knowing the scene information

The method was first proposed by Oakley and Satherley [87], who studied a degradation model that was based on multi-parameter statistics under the assumption that the depth of the scene is known, and then completed the scattering attenuation compensation using the estimated weights of pixel scattering and reflection, and obtained good recovery results. The method was only suitable for gray images when first proposed by Oakley; later, Tan *et al.* [89], [90] improved the algorithm by performing an in-depth study of the relationship between the quality of the image contrast and the wavelength, and extended the degraded image restoration to color images. On the basis of this study, Robinson *et al.* [91] constructed a dynamic and real-time weather system, which was based on the atmospheric scattering model to compensate for the loss of contrast by removing the environmental light components in each color channel.

Later, Hautière *et al.* [92] estimated the visibility distance using side geographical information that was obtained using an on-board optical sensor system [93], [94] to establish the relationship between the road visibility and the contrast in the foggy image [24]. They then computed the depth of the scene by modeling the depth value of each point as a Euclidean

distance function, and used the 3D geographical model to remove the fog. Kopf *et al.* [95] introduced a deep photo system that uses the existing digital terrain to provide the basic information. A three-dimensional model of the scene was built firstly by estimating a large amount of information such as depth and texture, and then the depth information values as well as the structure of the image colors and texture were determined in order to estimate a stable value for the curve haze. The final physical model can be used for the purpose of dehazing.

This method is based on the premise that the depth of the scene is known and that the restoration of the image is good. However, the hardware requirements for expensive radars and distance sensors and the requirement for an existing database to obtain accurate scene depth information severely limits the real-time applicability of this algorithm.

### b) User interaction

In addition, Narasimhan *et al.* [96] proposed a single foggy image interactive restoration method, which requires a user to input the area of the sky or the areas that are seriously affected by weather, the artificially-specified maximum depth of field and the minimum depth of the field area to obtain rough depth information. Using the estimation of scene depth map, the image is then restored based on the atmospheric scattering model. This method does not require precise information about the scene or the weather conditions, and does not require changes in weather conditions between image acquisitions. It is clear that such simple techniques are easy-to-use and can effectively restore clear daytime colors and contrasts from images taken in poor weather conditions, as shown by the example in Fig. 13. Sun *et al.* [97] later proposed a method that assumed gentle changes in the depth of the scene, and then simplified the atmospheric scattering model to a monochromatic model. With user assistance, the sky region and the maximum and minimum depth regions are obtained, and image dehazing is realized by solving the partial differential equation. This type of interaction based method can obviously improve the visual effects and contrast, but since it requires a certain degree of user interaction, it cannot be done automatically by a real-time system.

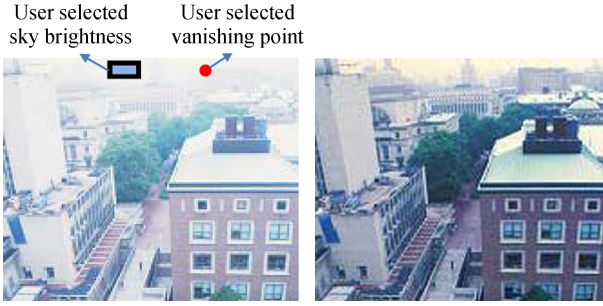


Fig. 13. User interaction dehazing method [96].

### c) Machine learning

In recent years, machine learning based methods have been used for foggy image dehazing [98]. Gibson *et al.* [99] explored the idea of learning the depth of fog from a given dataset and constructed an example based learning method that takes advantage of machine learning techniques as well

as knowledge of the physics of the atmosphere. Zhu *et al.* [100], [101] later proposed a simple and powerful method of prior color attenuation to create a linear model for scene depth of hazy images. In this method, a linear model is firstly created as follows.

$$d(x) = \theta_0 + \theta_1 v(x) + \theta_2 s(x) + \varepsilon(x) \quad (16)$$

where  $x$  is the position within the image,  $d$  is the scene depth,  $v$  is the brightness component of the hazy image,  $s$  is the saturation component,  $\theta_0, \theta_1, \theta_2$  are the unknown linear coefficients and  $\varepsilon(x)$  is the random error. Assuming a Gaussian density for  $\varepsilon$  with zero mean and variance  $\sigma^2$ , then according to the Gaussian distribution property,  $d(x)$  can be expressed as:

$$d(x) \sim p(d(x)|x, \theta_0, \theta_1, \theta_2, \sigma^2) = N(\theta_0 + \theta_1 v + \theta_2 s, \sigma^2). \quad (17)$$

By learning the parameters of the linear model with a supervised learning method on 500 training samples containing 120 million scene points, the bridge between the hazy image and its corresponding depth map can be effectively built with the best learning results such that  $\theta_0 = 0.121779$ ,  $\theta_1 = 0.959710$ ,  $\theta_2 = -0.780245$ ,  $\sigma = 0.041337$ . Using the recovered depth information, the haze can be easily removed from a single hazy image. The proposed approach runs quickly and can achieve good results, but the training procedure is complex and the parameters rely too much on the training data.

### 2) Multi-image Dehazing Methods

Depth or detailed information can also be estimated using two or more different images of the same scene. The recovery principles used by this method can be divided into two categories: different polarizing filters and different weather conditions.

#### a) Different polarizing conditions

A team of researchers led by Schechner *et al.* [102] have studied the polarized characteristics of light and found that reflected light from the target has no polarization characteristics, and sky light has some polarization characteristics after medium scattering. Therefore, using the polarization characteristics of sky light, the authors captured multiple images of the same scene with different polarization angles and obtained the degree of polarization, and then restored the degraded image.

In order to facilitate the description, eq. (14) can be updated as follows:

$$I = J_{\text{object}} e^{-\beta(\lambda)d} + A_{\infty} (1 - e^{-\beta(\lambda)d}) = J + A. \quad (18)$$

The basic process of image restoration by polarization of light is as follows.

Firstly, the degree of polarization (DOP) is defined as a global parameter, which is independent of the scene depth of the image. Set  $A^{\perp}$  and  $A^{\parallel}$  as the parallel component and the vertical component of atmospheric incident light ( $A^{\perp} > A^{\parallel}$ ) respectively, then, the DOP of atmospheric light can be expressed as:

$$P_A = \frac{A^{\perp} - A^{\parallel}}{A}. \quad (19)$$

Similarly, the light of the polarization imaging system can be decomposed into  $I^{\Pi}$  and  $I^{\perp}$  ( $I^{\perp} > I^{\Pi}$ ), and the DOP of the scene is defined as:

$$P_J = \frac{I^{\perp} - I^{\Pi}}{I}. \quad (20)$$

Since the two images in orthogonal polarization directions are  $I^{\Pi} = J/2 + A^{\Pi}$  and  $I^{\perp} = J/2 + A^{\perp}$ , then the intensity of the atmospheric light can be calculated:

$$A = \frac{I \times P_J}{P_A}. \quad (21)$$

Based on above equations, the dehazing image can be calculated using the formula:

$$J_{\text{object}} = \frac{I(1 - \frac{P_J}{P_A})}{1 - \frac{I \times P_J}{A_{\infty} \times P_A}}. \quad (22)$$

From the above analysis,  $P_J$  and  $I$  can be obtained by using two or more images in different polarization directions. If  $A_{\infty}$  and  $P_A$  are estimated by the polarized image in the infinity scene, then a clear image can be obtained from the fog. An example is shown in Fig. 14.

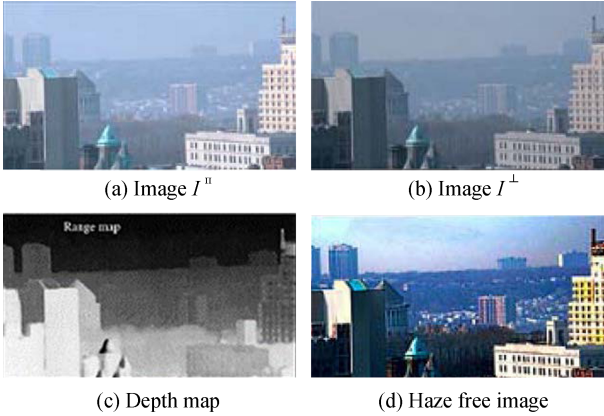


Fig. 14. Dehazing with polarized images [102].

Schechner *et al.* [102], [103] analyzed the imaging process of a foggy image, and explained the physical principle of the polarization effect based on atmospheric scattering. Firstly, two or more images were collected through adjusting the polarization direction of the polarizer; then, the contrast and correct colors of the scene were recovered using these obtained images in order to estimate the atmospheric optical polarization coefficient using this data. The optical depth of the scene is then obtained and image dehazing is realized using the atmospheric scattering physical model. Using these results, the scene depth map and the atmospheric particle properties can also be calculated. However, this method mainly depends on information about the infinite sky, so it has some limitations for application. Shwartz *et al.* [104] then proposed a type of blind classification method to solve the limitation of parameter estimation based on sky information. The sky information may be ignored by assuming that there is no correlation between the airlight component and the direct transmission component in some parts of the image, and an independent component analysis (ICA) method is adopted to restore the airlight component and other related data information in order

to improve the visibility and color of the image and achieve the purpose of dehazing. In addition, the authors also processed the noise added during the course of dehazing. After obtaining the distribution rate and the intensity of the ambient light, the noise is considered to be related to the distance and will be amplified when recovery occurs through the physical model. So the authors used the regularization method, adaptive weights related to distance [105] and the nano flow method [106] to remove noise.

In another paper [107], the authors proposed a type of polarimetric dehazing method to enhance the contrast and the range of visibility of images based on angle-of-polarization (AOP) distribution analysis. Reference [108] introduced an effective method to synthesize the optimal polarized-difference (PD) image and presented a new polarization hazy imaging model that considers the joint polarization effects of airlight and the object radiance in the imaging process. After analyzing several methods for estimating airlight parameters, reference [109] proposed blind estimation of the DOP based on independent component analysis (ICA). In the paper by Treibitz and Schechner [110], different angles of polarized filters are quantitatively analyzed according to their signal-to-noise ratio (SNR) to estimate the dehazing effects. A quality assessment method suitable for polarization analysis images in foggy conditions is proposed [111]. Reference [112] proposed a method that estimates the haze parameters from the polarization information of two known objects at different distances, and the estimated parameters are used to remove the haze effect from the image. Some methods can also be applied to underwater images [113]–[115], which can not only obtain clear images, but also enhance the structural information about the scene.

These methods are very dependent on the DOP of sky light. While they can enhance the image contrast under thin fog and dense fog, the dehazing effect may be greatly reduced because of inaccuracies in the scene information. In addition, it is difficult to find the maximum and minimum degrees of polarization under the same scene during rapid scene changes, and the operation is complicated, so it is not conducive to image restoration in real time.

#### b) Different weather conditions

Another method of obtaining depth information of a scene is by capturing two images of the same scene under different weather conditions. Narasimhan and Nayar [116]–[120] have extensively studied the extraction of depth information of a scene from different perspectives. By analyzing multiple obtained images of the same scene under different foggy conditions, it was found that under different scenarios, the intensity and color of the image was mainly determined by the atmospheric light and the scattering of atmospheric particles. Therefore, when there are multiple unknown parameters in the physical model, the authors combined two or more different degraded images to obtain useful information, proposed a geometric framework describing the impact of atmospheric scattering on color and used this framework for image dehazing. Firstly, the geometric constraints of color changes in different images is calculated; then, these constraints and the atmospheric scattering model are combined and the color and

depth information is computed; finally, a three dimensional structure is obtained to restore the clear image, which achieves good results. An example is shown in Fig. 15.

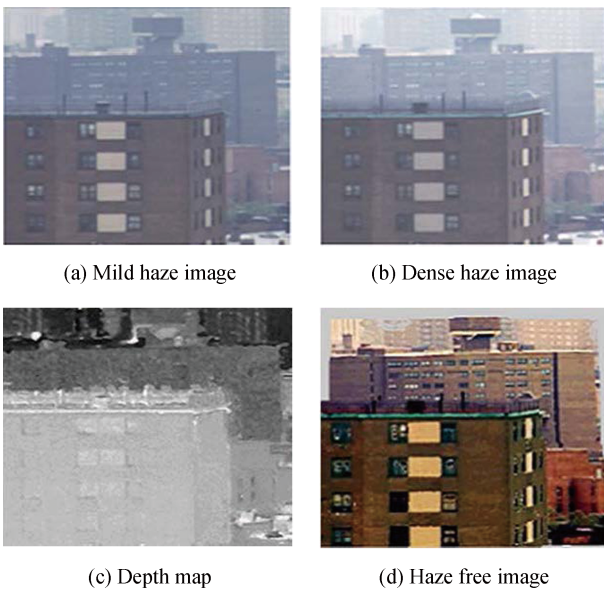


Fig. 15. Dehazing with polarized images [117].

Reference [116] analyzed the effects of the atmosphere on imaging and proposed a two-color atmospheric scattering model. The image degradation process due to atmospheric scattering was described as an interactive function of the color, the depth and the environmental light at particular points in the scene, and a structure of the fog concentration and image depth was constructed. The model takes into account the dependence of atmospheric scattering on wavelength, which requires a clear image of the scene without fog. In order to avoid this constraint, Narasimhan *et al.* [117] used color changes in the degraded images under different weather conditions as the constraint condition and proposed an effective algorithm for the reconstruction of a 3D scene structure including scene color information, which can be extended to color images. In [118], the method of constructing the depth information of the scene is described in detail which uses two images of the same scene with different weather conditions. Other reference [119], [120] introduced a method to calculate the scene structure, enhance the image contrast and restore clear images by searching for the depth of discontinuities.

Sun *et al.* [121] later improved the above method by changing the original distribution mode for the concentration, scattering coefficient and color information from global mode to local mode, where the gradient field related to the depth is obtained from the partial derivative of the atmospheric degradation equation, and the Poisson equation is solved to realize restoration of the foggy image. Chen *et al.* [122] used a foggy image and a clear image in the same scene as the samples to conduct optical modeling of the scene. After computing the depth ratio with corresponding points, the image was then restored with the atmospheric scattering model.

A data-driven approach was presented by Wu and Dai [123], where multiple observations of the same scene with various

levels of fog are obtained to estimate the scene depth, similar to the work of Nayar and Narasimhan [116]. Wu and Dai additionally provided a segmentation step to adapt to changes in a scene, such as planes moving across the field of view. Therefore, this approach can account for ambiguous regions.

These types of dehazing methods are simple and can achieve good results. However, two or more different images in the same scene are required, so it is difficult to realize image dehazing within a short time for real-time monitoring situations, and difficult to apply and popularize in practice.

### 3) Single Image Dehazing Method With Prior Knowledge

Single image dehazing is essentially an under-constrained problem. In order to make image dehazing more practical, some image dehazing methods based on additional priors or constraints have been proposed in recent years, adding new vitality to image processing [124]. Some classic algorithms of this type of method are introduced in the following paragraphs.

#### a) Tan method

In 2008, Tan [125] proposed an effective image dehazing method based on two prior conditions. The first condition is that the contrast in the image without fog should be higher than that of the foggy image. The second condition is that the attenuation of field spots is a continuous function of distance which should be smooth. The author firstly defined the color of light, and then by separating each color channel of the image brightness, the airlight color of the input image can be transformed to white. The equation can be modified as follows:

$$I'(x) = J'(x)t(x)' + A(x) \begin{bmatrix} 1 \\ 1 \\ 1 \end{bmatrix} \quad (23)$$

where  $I'(x)$  is the image after color standardization,  $J'(x)$  is the corresponding dehazed image, and the invariant  $A(x) = (A_r + A_b + A_c)(1 - t(x))$ .

Based on the first prior knowledge, the cost function of the edge strength is then constructed, and the formula can be expressed as:

$$C_{\text{edges}}(I) = \sum_{x,c} |\nabla I_c(x)| \quad (24)$$

where  $c \in \{R, G, B\}$  are RGB channels and  $\nabla$  is the differential operator.

Based on the second prior knowledge, the airlight is obtained using Markov random fields (MRFs). The potential function of the MRFs is:

$$E(\{A_x\} | P_x) = \sum_x \phi(P_x | A_x) + \eta \sum_{x,y \in N_x} \psi(A_x, A_y) \quad (25)$$

where  $\phi(P_x | A_x)$  is the data item,  $\psi(A_x, A_y)$  is the smooth item,  $P_x$  is the region with  $x$  as the center,  $A_x$  is the constant of the region,  $\eta$  is the strength of the smooth item and  $N_x$  is the neighbor of pixel  $x$ .

$A$  is finally obtained using the graph cut method to maximize the probability of a Gibbs distribution, and it is used to calculate the transmission rate for the image restoration.

This method can realize dehazing by maximizing the local contrast with only one image. However, serious “halo” effects

can easily occur due to sudden changes of depth, leading to color oversaturation in images with heavy haze.

Based on the same assumption [126], Ancuti *et al.* later proposed another dehazing technique which is optimized to preserve the original color spatial distribution and local contrast that is suitable for the challenging problem of image matching based on local feature points.

In order to address the over-enhancing effects of the Tan method, and inspired by the Bertalmío method [127], Galdran *et al.* proposed a perception-inspired variational framework [128], [129] for the task of single image dehazing without requiring the depth structure of the scene to be estimated. The method performs a spatially-variant contrast enhancement that effectively removes haze from far away regions.

### b) Fattal method

Based on the prior knowledge that there is no correlation between object surface shading and the transmission map, Fattal [130] used independent component analysis (ICA) and a Markov random field (MRF) model to estimate the surface albedo, then obtained the medium transmission of the scene and recovered the clear image from the foggy image. The key steps can be described as follows:

Firstly, each pixel in the unknown clear image  $J$  is modeled as the product of the surface reflection coefficient  $R$  and a shadowing factor  $l$ , i.e.  $J = Rl$ . Therefore, equation (15) can be transformed to:

$$I(x) = t(x)l(x)R + (1 - t(x))A \quad (26)$$

$R$  is then decomposed into two components. The first component is parallel to the direction of atmospheric light,  $A$  and the second component is called residual vector the  $R' \in A_{\perp}$  and is perpendicular to the direction of  $A$ . Therefore, the transmission can be calculated using the formula:

$$t(x) = 1 - (I_A(x) - \eta I_{R'}(x)) / \|A\| \quad (27)$$

where  $I_A(x)$  and  $I_{R'}(x)$  are the projections of the input image along the  $A$  direction and  $R'$  direction, respectively,  $\eta = \langle R, A \rangle / (\|R'\| \|A\|)$  is the measurement of atmospheric light and  $\langle \cdot, \cdot \rangle$  is the standard 3D point multiplication in RGB space.

Finally, the foggy image is recovered through an inverse process of the image degradation model with the transmission function.

This approach is physically sound and can usually produce impressive results when there is sufficient color information. Nevertheless, it cannot effectively restore images with heavy haze and may fail in cases where the original assumptions are invalid.

In a subsequent work [130], the same author Fattal [131] presented another new single-image dehazing method based on the color-line pixel regularity in natural images, and also proposed an augmented GMRF model with long-range coupling in order to more accurately resolve the transmission in isolated pixels lacking their own estimates.

### c) Kratz method

Kratz *et al.* [132] proposed another approach that is related to the Tan method [125], which assumes that the foggy image is composed of albedo and depth in independent latent layers,

and the factorial Markov random field (FMRF) is used to compute the depth information in order to recover the haze-free image.

In this literature, eq. (15) is deformed as follows:

$$\ln(L_{\infty}^{-1}I(x) - 1) = \ln(\rho(x) - 1) - \beta d(x) \quad (28)$$

where  $\rho(x)$  is the albedo information and  $d(x)$  is the depth information.

Setting  $\tilde{I}(x) = \ln(L_{\infty}^{-1}I(x) - 1)$ ,  $C(x) = \ln(\rho(x) - 1)$  and  $D(x) = -\beta d(x)$ , (28) can be expressed as:

$$\tilde{I}(x) = C(x) + D(x) \quad (29)$$

where  $C(x)$  and  $D(x)$  represent the scene albedo item and the scene depth item and it can be assumed that both are independent statistically. If  $p(C)$  and  $p(D)$  are the prior knowledge, then,  $C(x)$  and  $D(x)$  can be computed through the maximum posterior probability:

$$\arg \max_{\tilde{\rho}, \tilde{d}} p(C, D | \tilde{I}) = \arg \max_{\tilde{\rho}, \tilde{d}} p(\tilde{I} | C, D) p(C) p(D). \quad (30)$$

Kratz's method can recover a haze-free image with fine edge details, but the results are often over-enhanced and suffer from oversaturation.

The technique of Kratz and Nishino [132] was later extended in [21]. Kratz *et al.* [132] introduced a novel Bayesian probabilistic method that jointly estimates the scene albedo and depth from a single degraded image by fully leveraging its latent statistical structures. Their approach models the image with a factorial Markov random field (FMRF) by jointly estimating two statistically independent latent layers for the scene albedo and depth. Experimental results show that the method can achieve good results but the technique produces some dark artifacts in regions approaching infinite depth.

Similar to the MRF model in [133], Caraffa and Tarel [134], [135] took advantage of both stereo and atmospheric veil depth cues to achieve better stereo reconstructions in foggy weather and proposed a Markov random field model of the stereo reconstruction and defogging problem. Their method can be optimized iteratively using an  $\alpha$ -expansion algorithm. Based on the Bayesian framework, Nan *et al.* [136] proposed a method for single image dehazing taking noise into consideration, and obtained the reflectance image using an iterative approach with feedback to obtain a balance between dehazing and denoising. In order to reduce the computation time of [133], Mutimbu *et al.* [137] considered the defogging problem as a relaxed factorial Markov random field (FMRF) of albedo and depth layers, which can be efficiently solved using sparse Cholesky factorization techniques. Rather than factorizing the scene albedo and depth through a log-transform, Dong *et al.* [138] introduced a sparse prior and an additive noise argument in the degraded image model, and proposed an alternative optimization method to iteratively approximate the maximum a posteriori (MAP) estimators of these variables. Zhang *et al.* [139], [140] later described a new framework for video dehazing based on the Markov random field and optical flow estimation, which builds an MRF model on the transmission map to improve the spatial

and temporal coherence of the transmission. Exploring this in further depth, Wang *et al.* [141] proposed a multi-scale depth fusion (MDP) scheme which obtains the depth map of the physical model using an inhomogeneous Laplacian-Markov random field (ILMRF), which can better estimate the depth map while accommodating the advantages of different patches and reducing the drawbacks of other methods.

#### d) He method

He *et al.* [142], [143] proposed a dark channel prior (DCP) algorithm that can effectively overcome the deficiencies of the above two algorithms (Tan [125], Fattal [130]) to some extent. The dark channel principle is sourced from a remote sensing image and an underwater image is used to summarize the rules from a natural image with no fog. The authors then combined the principle with the atmospheric scattering model and realized single image dehazing based on DCP. The motivation of DCP is that for most non-sky patches in haze-free outdoor images, at least one color channel has very low intensity for some pixels, with a brightness value  $J^{\text{dark}}(x)$  that is close to 0. It can be expressed as:

$$J^{\text{dark}}(x) = \min_{y \in \Omega(x)} \left( \min_{c \in \{r,g,b\}} (J^c(y)) \right) \rightarrow 0 \quad (31)$$

where  $J$  is the haze-free image and  $\Omega(x)$  is the local patch with pixel  $x$  at the center.

Using this priori, He *et al.* were able to identify the local dark channel patches in the image and used these to roughly estimate the atmospheric transmission. Thus the atmospheric scattering model (15) can be transformed into:

$$\begin{aligned} \min_{y \in \Omega(x)} \left( \min_c \left( \frac{I^c(y)}{A^c} \right) \right) &= \tilde{t}(x) \min_{y \in \Omega(x)} \left( \min_c \left( \frac{J^c(y)}{A^c} \right) \right) \\ &\quad + (1 - \tilde{t}(x)). \end{aligned} \quad (32)$$

Based on the DCP (32), the rough transmission map  $\tilde{t}(x)$  can then be obtained:

$$\tilde{t}(x) = 1 - \min_{y \in \Omega(x)} \left( \min_c \left( \frac{I^c(y)}{A^c} \right) \right). \quad (33)$$

If the atmospheric scattering model is directly inverted to obtain the haze-free image, there will be a significant block effect on the transmission map. Therefore, the authors optimized their method using soft matting [144]. The optimal  $t(x)$  can be obtained by solving the following sparse linear system:

$$(L + \lambda U)t(x) = \lambda \tilde{t}(x). \quad (34)$$

The matrix  $L$  is called the matting Laplacian matrix.  $\lambda$  is set to  $10^{-4}$  and  $t(x)$  is softly constrained by  $\tilde{t}(x)$ .

The DCP algorithm is an important breakthrough in the field of single image dehazing. Gibson and Nguyen [145], [146] described the effectiveness of this approach using principal component analysis and minimum volume ellipsoid approximation, and Tang *et al.* [98] confirmed that the dark-channel feature is the most informative feature for dehazing from a learning perspective. DCP provides a new concept for researchers, but refinement of its transmission map requires high computations. Additionally, when the image contains large bright areas such as sky, water or white objects, the dark channel prior assumptions will be invalid.

Many improvements were later done to refine the coarse transmission map based on DCP, such as WLS edge-preserving smoothing [147], bilateral filtering [148]–[150], a fast O(1) bilateral filter [151], joint bilateral filtering [152], a joint trilateral filter [153], guided image filtering [6], [154]–[160], weighted guided image filtering [161], [162], content adaptive guided image filtering [163], smooth filtering [164], anisotropic diffusion [165], window adaptive method [166], associative filter [167], edge-preserving and mean filters [168], a joint mean shift filtering algorithm [169], adaptively subdivided quadtree [170], edge-guided interpolated filter [171], an adaptive Wiener filter [172], guided trigonometric bilateral filters [32], median filter and gamma correction [173], Laplacian-based gamma correction [174], fuzzy theory and weighted estimation [175], opening operation and fast joint bilateral filtering [176], cross bilateral filtering [177] and a fusion strategy [4], [86], [178], [179] to optimize the transmission image.

Some approaches have also been proposed based on improved DCP. In [9], a median DCP (MDCP) algorithm was proposed in order to improve He's transmission model [142]. By calculating the median neighborhood instead of the minimum value of the DCP algorithm, the halo phenomenon appearing at the edge of the scene is reduced. Shiau *et al.* [180] applied a weighted technique to estimate the atmospheric light and transmission. The method mitigates halo artifacts around the sharp edges and computes the transmission map adaptively using a trade-off between the  $1 \times 1$  pixels and the  $15 \times 15$  pixel dark channel maps. While this method can preserve edges, it generates oversaturation.

Based on the observation that areas with dramatic color changes tend to have similar depths, a window variation mechanism was proposed in another paper [181] that uses the neighborhood scene complexity and the color saturation rate to achieve an ideal compromise between depth resolution and precision.

The other issue is the invalidity of DCP when other objects have similar colors as the atmospheric light. The method proposed in [182] defines a reliability map that depicts how many objects or areas meet the dark channel prior assumption, and then estimates the transmission map using the reliable pixels only. Wang and Zhu [183] introduced a novel variational model (VM) to optimize the transmission using a smoothness term and a gradient-preserving term to prevent false edges and distorted sky areas in the recovered image.

Later, Meng *et al.* [184] provided a new geometric perspective for DCP using a boundary constraint, and proposed a transmission image optimization algorithm that explores the boundary constraint and contextual regularization. This method is fast and can attenuate image noise and enhance some interesting image structures. Chen *et al.* [185] proposed an approach based on Bi-Histogram modification that exploits the features of gamma correction and histogram equalization to flexibly adjust the haze thickness in the transmission map of DCP. Reference [186] later presented a new image haze removal approach that can solve the problems associated with the presence of localized light sources and color shifts, which was based on Fisher's linear discriminant-based dual dark

channel prior scheme.

Motivated by DCP, Ancuti *et al.* [187] proposed a semi-inverse (SI) method of converting the image to LCH (lightness, chroma and hue) space by using the inverse operator for fast dehazing, which reduces the complexity of He *et al.*'s [142] algorithm by converting the approach from block-based to layer-based. Gao *et al.* [188] later combined DCP to present a fast image dehazing algorithm based on negative correction to improve the perceptual quality while reducing the computational complexity. Rather than estimating the transmission map, the correction factor of the negative of the images is estimated and used to rectify the corresponding hazy images. Li *et al.* [189] proposed a luminance reference model for transmission estimation by searching for the lowest intrinsic luminance with small sliding windows, and then refined it utilizing a bilateral filter to smooth out noises and obtain a reliable result.

Additionally, DCP-based methods have been extended for use to night-time images [190]–[192], underwater images [31] and rainy or snowy [39] conditions. For example, in order to improve the robustness of the DCP algorithm for night-time hazy images, Pei *et al.* [190] combined a color transfer method which transformed the airlight colors from a “blue shift” to “grayish”, and then used a DCP method to remove night-time haze. Their method can achieve results with more details but the color characteristics of the input are also changed by the color transfer procedure. Therefore, reference [191] presented a new imaging model for night-time haze conditions, which takes into account both the non-uniform light conditions and the color characteristics of artificial light sources, achieving both illumination-balance and haze free results. Reference [192] presented an improved DCP model which was integrated with local smoothing and image Gaussian pyramid operators to enhance the perceptual quality of the night videos. For underwater images, reference [31] proposed an underwater DCP (UDCP) methodology which basically considers blue and green color channels to be the underwater visual information source. This method provides a significant improvement over existing methods based on DCP.

#### e) Tarel method

Tarel *et al.* [193] introduced a contrast-based enhancement approach to remove haze effects, which aims to be faster than previous approaches. It assumes that the atmospheric veil function changes gently over a local region, so the transmission coefficient of the medium can be estimated by pretreatment and median filtering. Firstly, a white-balancing operation is applied to the foggy image, and the foggy regions are regulated to white. Then, the atmospheric scattering model given by (15) is transformed to:

$$I(x) = J(x)(1 - A^{-1}V(x)) + V(x) \quad (35)$$

where  $V(x) = A(1 - t(x))$  is the atmospheric veil function.

The minimum color components  $W(x)$  of the input image  $I(x)$  can be calculated by:

$$W(x) = \min_c(I(x)), \quad c \in \{r, g, b\}. \quad (36)$$

In order to handle edge contours which cause sudden changes in depth in the image, median filtering is performed on  $W(x)$  to obtain  $B(x)$  with a window size  $sv$ .

$$A(x) = \text{median}_{sv}(W(x)) \quad (37)$$

$$B(x) = A(x) - \text{median}_{sv}(|W(x) - A(x)|). \quad (38)$$

Then, the atmospheric veil function can be calculated.

$$V(x) = \max(\min(pB(x), W(x)), 0) \quad (39)$$

where  $p$  is the adjusting factor of the dehazing degree.

After solving  $V(x)$ , the haze free image  $J(x)$  is revealed through (35).

The Tarel method greatly simplifies the dehazing process and improves efficiency, and Gibson *et al.* [194] used the color ellipsoid framework to explain its principle. However, after median filtering, the smoothed atmospheric veil did not maintain the depth edge information, so the algorithm is sometimes invalid in small edge regions. There are many parameters in the algorithm, which cannot be adjusted adaptively.

Based on Tarel *et al.*'s method [193], Yu *et al.* [195] proposed an edge-preserving smoothing approach based on a weighted least squares (WLS) optimization framework to smooth the edges of image. Bilateral filtering [196] has also been used to refine the atmospheric veil function estimation. Zhao *et al.* [197] proposed another edge-preserving smoothing approach based on local extremes to estimate the atmospheric veil, finally applying the inverse scene albedo for the recovery process. Xiao *et al.* [198] later improved Yu *et al.*'s [195] method further by combining joint bilateral filtering [199], and proposed a guide joint bilateral filter to refine the transmission map obtained by median filtering. This method can preserve edges and reduce the computation complexity to  $O(N)$ . Bao *et al.* [200] proposed an edge-preserving texture-smoothing filtering method to improve the visibility of images in the presence of haze or fog. Their method can effectively achieve strong textural smoothing while maintaining sharp edges, and any low-pass filter can be directly integrated into the framework. Based on Tarel's framework, reference [201] later introduced non-local structure-aware regularization to properly constrain the transmission estimation without introducing halo artifacts.

Due to the properties of the median filter, the results of Tarel's work cannot remarkably preserve the edges and gradients of the images and may cause halo artifacts around objects. Thus, reference [202] introduced a digital total variation filter with color transfer (DTVFCT) for single color image dehazing. The estimation of the atmospheric veil is a filtering problem on the minimal component image and a digital TV filter is applied to preserve the edges and gradients of the images, in order to avoid halo artifacts. Negru *et al.* [203] proposed an efficient single image enhancement algorithm that is suitable for daytime fog conditions, which take the exponential decay present in foggy images into account when computing the atmospheric veil. Li *et al.* [204] presented a change of detail (CoD) prior in an image model, which can estimate the atmospheric veil through a sharper operator and a smoothing operator effectively to recover the haze-free image.

### f) Kim method

In order to maintain a balance between avoiding overstretching the contrast [125], [132], [142], [193] and the inability to remove dense haze [130] because of incorrect estimation of scene depths, Kim *et al.* [158], [205] presented a dehazing algorithm based on optimized contrast enhancement by maximizing the block-wise contrast while minimizing the information loss due to pixel truncation. Using a temporal coherence measure, the algorithm has been extended for video dehazing.

Firstly, the atmospheric light in a hazy image is selected using the quad-tree based subdivision.

The scene depths are then assumed to be locally similar and the haze equation, equation (15) can be rewritten as

$$J(x) = \frac{1}{t} (I(x) - A) + A. \quad (40)$$

The contrast cost  $E_{\text{contrast}}$  and the information loss cost  $E_{\text{loss}}$  of each block  $\Omega$  are then defined as:

$$E_{\text{contrast}} = - \sum_{c \in \{r,g,b\}} \sum_{x \in \Omega} \frac{(I_c(x) - \bar{I}_c)^2}{t^2 N} \quad (41)$$

$$\begin{aligned} E_{\text{loss}} = & \sum_{c \in \{r,g,b\}} \left\{ \sum_{i=0}^{\alpha_c} \left( \frac{i - A_c}{t} + A_c \right)^2 h_c(i) \right. \\ & \left. + \sum_{i=\beta_c}^{255} \left( \frac{i - A_c}{t} + A_c - 255 \right)^2 h_c(i) \right\} \end{aligned} \quad (42)$$

where  $\bar{I}_c$  and  $N$  are the average values of  $I_c(x)$  and the number of pixels in  $\Omega$ ,  $h_c(i)$  is the histogram of the input pixel value  $i$  in the color channel  $c$ , and  $\alpha_c$  and  $\beta_c$  denote truncated values due to underflow and overflow, respectively.

Finally, for block  $\Omega$ , the optimal transmission  $\tilde{t}$  can be obtained by minimizing the overall cost function:

$$E = E_{\text{contrast}} + \lambda_L E_{\text{loss}} \quad (43)$$

where  $\lambda_L$  is a weighting parameter.

Experimental results have demonstrated that the proposed algorithm is capable of effectively removing haze and faithfully restoring images, as well as achieving real-time processing. However, it is not suitable for image dehazing in thick fog.

Similar to Kim's method, reference [206] later used local atmospheric light to estimate the transmission for each local region using an objective function represented by a modified saturation evaluation metric and an intensity difference, consisting of image entropy and information fidelity [207]. Motivated by this, Lai *et al.* [208], [209] assumed that the transmission map is under a locally constant variable, and proposed an optimal transmission map method using an objective function, which guarantees a global optimal solution. The obtained transmission map accurately preserves the depth consistency of each object.

#### 4) Atmospheric Light Estimation

Most of the present methods are targeted mainly at improving the quality of the estimated transmission, while often computing rough estimates of the atmospheric light. In fact, the atmospheric light estimation is as important as the transmission estimation, and an incorrect atmospheric light calculation can cause a dehazed image to look unrealistic. However, there are some methods that can be used to address this problem.

Narasimhan *et al.* [96] adopted a direct manual method to define image regions affected by atmospheric light, but it is not applicable to realistic application due to frequent interruption. Nayar *et al.* [116] and Kratz *et al.* [132] employed a method to estimate atmospheric light by selecting a patch of the sky in the foggy image. Their methods can achieve good estimation and have been used in some following algorithms. However, the methods only work if there is sky in the scene. Narasimhan *et al.* [117] and Fattal [130] calculated the direction of atmospheric light, but it was hard to determine the intensity of the light. Fattal [130] applied the principle of uncorrelation to search within small windows of constant albedo for white pixels that have the lowest correlation. However, over-saturation may occur when there are white objects with high intensities. In [141], the authors assumed that fog-opaque pixels exist not only in the deepest regions of the depth map but also in smooth regions of foggy images, since fog-opaque regions exhibit atmospheric luminance and conceal the textured appearance of the scene. All pixels in the fog-opaque region are averaged to obtain the color vector of the atmospheric luminance. In the work of Tan *et al.* [125], the brightest pixels in the hazy image were used as the atmospheric light. However, when there is a white object in the image, this method is not appropriate. He *et al.* [143] used the pixels with the highest intensity in the hazy image, e.g., the top 0.1% of the brightest pixels was selected from the dark channel. However, this method is also influenced by white objects. Tarel *et al.* [193] estimated the atmospheric light by calibrating the white balance of the image. This method is simple to operate and works well for most practical scenes. Kim *et al.* [158] selected the atmospheric light in a hazy image using a hierarchical searching method based on quad-tree subdivision, which repeats the steps in order to divide it into four rectangular regions. The brightest region is chosen as the atmospheric light according to a threshold. This method is simple and reliable. Pedone *et al.* [210] proposed a method based on novel statistics gathered from natural images regarding frequently occurring air-light colors, which used statistics to design a new robust solution for computing the color hue of the air-light. This method is easy to compute. In contrast with previous methods that focus on luminance estimation, Cheng *et al.* [211] proposed a linear time atmospheric light estimation algorithm based on color analysis, by estimating the color probability in YCbCr space to select candidates from the representative fog pixels for air-light color computation. This method is effective and has very low computation cost.

In summary, although atmospheric light is an important parameter for restoration based image dehazing, there are not as many algorithms proposed to estimate the atmospheric light

as there are for estimating the transmission map.

### III. QUALITY ASSESSMENT FOR IMAGE DEHAZING

Image quality assessment (IQA) is an essential step in image dehazing. Generally speaking, the assessment of image quality includes two main aspects: image fidelity and image readability which can be classified as the subjective assessment and the objective assessment.

#### A. Subjective Assessment

The subjective assessment method uses observers to make the quality assessment using a set of assessment criteria according to their visual opinion of the processed image. The results are summarized to compare the performance of the algorithm. The score was divided into 5 grades. The assessment required that there were more than 20 assessors and that some people have experience in image processing while others should have no knowledge of image processing. The final quality score, called the mean opinion score (MOS), is computed to obtain the overall assessment score by averaging the subjective scores from all assessors. The assessment criteria are shown in Table I.

TABLE I  
THE CRITERIA OF SUBJECTIVE ASSESSMENT

Score	Assessment grade	Quality criteria
1	Worst	The worst in the group
2	Worse	Worse than average
3	Average	Average in the group
4	Better	Better than average
5	Best	The best in the group

Although this method is simple and can reflect the visual quality of the image, it lacks stability and is often subject to experimental conditions, the knowledge of the observers, their emotions, motivation, and many other factors. In the current literature, the most common existing solution is to manually present several images in bad visibility alongside their corresponding enhanced images which have been processed by different algorithms, and then enlarge some regions with key details for subjective comparison. This method lacks consistency from different assessors, and is difficult to use in engineering applications.

#### B. Objective Assessment

The objective assessment method evaluates the image with qualitative data according to objective criteria. In general, there are three major categories of quantitative metrics depending on the availability of an original image: full-reference methods, reduced-reference methods and no-reference methods, with the first two categories needing to use a reference image. However, for image dehazing, the reference image of the same scene without haze is usually very difficult to obtain, so there is no ideal image to be used as a reference. Therefore, the no-reference evaluation method is often used or a dehazed image is used as the reference image to evaluate the performance of the algorithms.

At present, the dehazed image assessment methods can be divided into two categories in this paper according to their special purpose: ordinary method and special method. The former is a general method used for evaluating the quality of any image, which is adapted to evaluate dehazing effects only; and the latter is specially designed for use in the dehazing applications, which uses an assessment principle that is combined with the characteristics of the hazy conditions.

#### 1) Ordinary IQA

As can be seen from [187], [212], many general IQA have been employed for image dehazing applications, such as Aucuti *et al.* [187] who have compared images with radically different dynamic ranges [212] to evaluate both the contrast and the structural changes. Liu *et al.* [178] adopted a color naturalness index (CNI) and a color colorfulness index (CCI) [213] for algorithm evaluation and analysis. Wang *et al.* [179] considered that images captured in hazy weather often suffer from a degradation in contrast, color distortion, and missing image content, then applied an average gradient (AG), a color consistency (CC) [214] and a structure similarity (SSIM) for objective evaluation. Ma *et al.* [215] adopted eight dehazing algorithms to perform image dehazing on 25 images, then evaluated the quality through subjective users and some general IQA methods (BIQI [216], BRISQUE [217], NIQE [218], BLINDS-II [219], DILT [220] and NCDQI [221]) and concluded that none of these IQA models properly predicts the perceived quality of dehazed images. Some of the commonly-used IQAs for dehazing images are introduced as follows:

a) *Standard deviation (STD)*: The STD reflects the degree of dispersion in the image relative to its average value, and is a measure of the contrast in a certain range. The larger the standard deviation, the better the visual effect will be:

$$\delta = \sqrt{\frac{1}{M \times N} \sum_{i=1}^M \sum_{j=1}^N (f(i, j) - \mu)^2} \quad (44)$$

where  $M$  and  $N$  are the width and the height of the image, respectively;  $f(i, j)$  is the gray value of pixel  $(i, j)$  and  $\mu$  is the average value of the whole image.

b) *Mean gradient (MG)*: The average gradient reflects the ability to express details of an image [164] and can be used to measure the relative clarity of the image. It is formulated as

$$G = \sqrt{\frac{1}{M \times N} \sum_{i=1}^{M-1} \sum_{j=1}^{N-1} ((f(i, j) - f(i+1, j))^2 + (f(i, j) - f(i, j+1))^2)} \quad (45)$$

where  $M$  and  $N$  are the width and the height of the image, respectively, and  $f(i, j)$  is the gray value of pixel  $(i, j)$ .

c) *Information entropy (IE)*: If an image is taken as a source of random output sets  $\{a_i\}$  and the probability of  $a_i$  is  $P(a_i)$ , then the average amount of information in the image is as follows:

$$H = - \sum_{i=1}^L P(a_i) \log_2 P(a_i). \quad (46)$$

According to the theory of entropy, the larger the value of IE, the more information is in the image.

d) *Mean squared error (MSE)*: The simplest and most widely used full-reference quality metric which is computed by averaging the squared intensity differences of the distorted and reference image pixels [98], [101], [164]. It is formulated as

$$MSE = \frac{1}{M \times N} \sum_{i=1}^M \sum_{j=1}^N [f(i, j) - f'(i, j)]^2 \quad (47)$$

where  $M$  and  $N$  are the width and the height of the image, respectively,  $f(i, j)$  is the original image and  $f'(i, j)$  is the dehazed image.

e) *Peak signal to noise ratio (PSNR)*: The PSNR can be used as an index of the signal distortion. A large PSNR corresponds to a smaller image distortion [141], [153], [164]. It can be expressed as:

$$PSNR = 10 \lg \frac{f_{\max}^2}{MSE} \quad (48)$$

where  $f_{\max}$  is the largest gray value, in general  $f_{\max} = 255$ .

f) *Structural similarity (SSIM)*: Generally, the human visual perception is highly adapted to extracting structural information from a scene. So, Wang *et al.* [222] proposed an SSIM index method to measure the restored image quality from the perspective of image formation, using the three components of luminance comparison  $l(x, y)$ , contrast comparison  $c(x, y)$  and structural comparison  $s(x, y)$ . The three components are combined to yield an overall similarity measure. Its formula is as follows:

$$S(i, j) = F(l(x, y), c(x, y), s(x, y)). \quad (49)$$

A diagram for the SSIM measurement system is shown in Fig. 16.

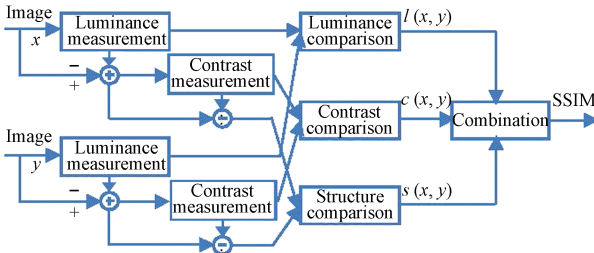


Fig. 16. Diagram of the SSIM measurement system.

The similarity of the two images is dependent on SSIM, and has a value between [0,1]. When the value is close to 1, the two images are more similar. This method can effectively simulate the human eye to extract structural information from the image, and the evaluation results are very close to the human eye. This method has been used in many studies to evaluate the performance of dehazing methods [101], [141], [153], [179], [183].

STD reflects the contrast of the image; IE reflects the information contained in the image; AG reflects the clarity of the image; and MSE, PSNR and SSIM reflect the degree of distortion of an image. For MSE, PSNR and SSIM, foggy images are usually adopted as references, because no fog-free images exist in these benchmark data. Higher MSE, lower PSNR and SSIM scores imply greater dissimilarity between restored results and referenced foggy image. The

above measures are often used for simple calculation since they have clear physical meaning and are mathematically convenient in the context of optimization. However, unfortunately these approaches cannot be simply adopted, because existing IQA metrics are generally inappropriate for this application since they are designed to assess distortion levels rather than the visibility of fog in images which may not be otherwise distorted.

### 2) Special IQA

Some IQAs have been designed particularly for use in image dehazing from different views. These IQAs are introduced as follows.

#### a) Visible edge based method

At present, within research on dehazing effect assessment, the most famous approach is a blind contrast enhancement assessment approach proposed by Hautière *et al.* [223], which is mainly based on an atmospheric luminance model and the concept of a visibility level, which is usually used in lighting engineering. The method evaluates the contrast enhancement detail between a hazy image and a haze-free image with three indexes:  $e$  (the rate of new visible edges),  $\bar{r}$  (the ratio of the gradient of the visible edges before and after restoration) and  $\sigma$  (the ratio of saturated (black or white) pixels).

$$e = \frac{n_r - n_0}{n_0} \quad (50)$$

$$\bar{r} = \exp \left( \frac{1}{n_r} \sum_{P_i \in \Psi_r} \log r_i \right) \quad (51)$$

$$\sigma = \frac{n_s}{\dim_x \times \dim_y} \quad (52)$$

where  $n_0$  and  $n_r$  are the number of visible edges before and after dehazing,  $\Psi_r$  is the visible edge sets of the dehazed image,  $P_i$  are the pixels of the visible edges,  $r_i$  is the Sobel gradient ratio of  $P_i$  and the corresponding points of the original image,  $n_s$  is the number of saturated pixels (black and white) and  $\dim_x$  and  $\dim_y$  denote the width and the height of the image respectively. The larger that  $e$ , or  $\bar{r}$  are and the smaller that  $\sigma$  is, the better the dehazing performance will be.

This method can efficiently reflect the edge details of the images before and after dehazing [80], [83], [173]–[175], [177], [178], and it is used for dehazing method evaluation [189], [197], [203], [204], [206], [224]. However, it only provides three indices for evaluation rather than a generalized assessment result, and sometimes the evaluation results will be inconsistent. The method also cannot evaluate the color distortion.

#### b) Color distortion based method

To address the color distortion problem due to halo artifacts and color shifts, Li *et al.* [225] proposed a color quality assessment of dehazed images based on a color histogram, histogram similarity and a color recovery coefficient. The original image and the dehazed image are decomposed into an illumination component and a reflection component using a Gauss low-pass filter. Detailed intensity detection, color recovery detection and scene structure detection are then performed and finally the recovery coefficient of the dehazed image is obtained. The diagram is shown in Fig. 17.

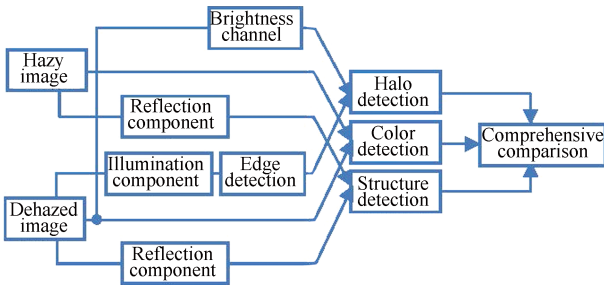


Fig. 17. The diagram of an assessment system based on color distortion.

This approach can reasonably assess the degree of color recovery in the dehazed image based on visual differences in the images before and after dehazing, by calculating the similarity coefficient of the two histogram distributions. However, it ignores the evaluation of color richness and a complex computation problem exists.

#### c) Contrast-naturalness-colorfulness (CNC) assessment

Guo *et al.* [226] later proposed a CNC assessment system which combines contrast, color naturalness and colorfulness. The diagram is shown in Fig. 18. This evaluation system is designed to detect contrast and the color quality of the image based on the visual perception of human eyes. Firstly, the contrast enhancement degree  $e$  is computed using the visible edges from images before and after dehazing; then, the color natural index (CNI) and the color colorfulness index (CCI) are obtained from the dehazed image. Finally, a comprehensive evaluation function is constructed using  $e$ , CNI and CCI, and the restoration performance of each dehazing method is evaluated objectively and quantitatively.

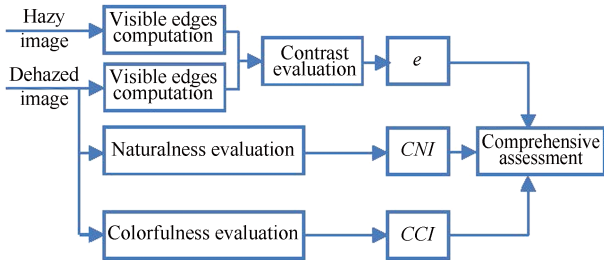


Fig. 18. Diagram of CNC assessment system.

Although this method gives assessment results that are close to the visual perception of human eyes, the evaluation process is complex and the evaluation results depend too much on the selection of parameters.

#### d) Machine learning-based method

More recently, Chen *et al.* [227] considered the IQA task to be a classification problem and exploited a rank SVM to learn a quality predictor in order to compare image enhancement algorithms for foggy images, underwater images and low light images. Their approach is focused on the relative quality ranking between enhanced images rather than assigning an absolute quality score for a single enhanced image. First, the authors constructed a dataset which contains source images under bad visibility and their enhanced images processed by different enhancement algorithms. Then, a subjective assessment is then performed in a pair-wise way to obtain the relative ranking of these enhanced images. Finally, a rank function is trained to

fit the subjective assessment results, and can be used to predict the ranks of new enhanced images, thus indicating the relative quality of the enhancement algorithms. The framework of this method is shown in Fig. 19.

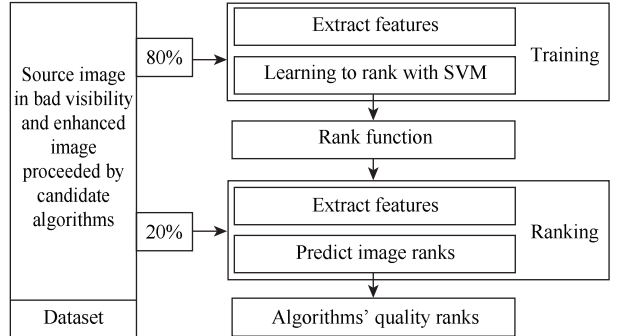


Fig. 19. The machine learning-based method.

The experimental results have shown that the proposed approach statistically outperforms state-of-the-art general purpose NR-IQA algorithms for image dehazing. However, inevitably for machine learning based methods, images processed from different sources usually do not share the same classification criterion.

### C. Experimental Results Evaluation

In order to compare the effects of various algorithms and to test the consistency of subjective and objective evaluation criteria, several dehazing methods have been selected to undergo quality evaluation algorithms. The “Mountain” image and the “New York” image are used as the original experimental images and are listed in Fig. 20 (a). Fig. 20 gives the comparison of the experimental results for various methods including gray-scale stretching, histogram equalization, adaptive histogram equalization, the Retinex method, homomorphic filtering, the wavelet transform, the Tan method [125], the Kopf method [95], the Fattal method [130], the Tarel method [193], the He method [142], the Meng method [184], the Kim method [158], and the Zhu method [101].

As can be seen from Fig. 20 (b)–(g), all of the image enhancement methods improve the visual effects of the original image to some extent with the exception of Fig. 20 (g), which may be due to unreasonable wavelet coefficient resulting in blur in this image. In Fig. 20 (b) and (f) have little tone shifting overall, but still do not have an ideal improvement effect. In Fig. 20 (b), the gray-scale stretching results in the loss of some details and the contour of cloud becomes vague, and in Fig. 20 (f), the homomorphic filtering method results in a darker color with a lower contrast in the image, but it achieves the best visual effect of these two images over the other image enhancement methods. In contrast, the image restoration methods obviously improve the hazy image in terms of both tone and detail recovery, and the visual effect is obviously better than the above image enhancement methods.

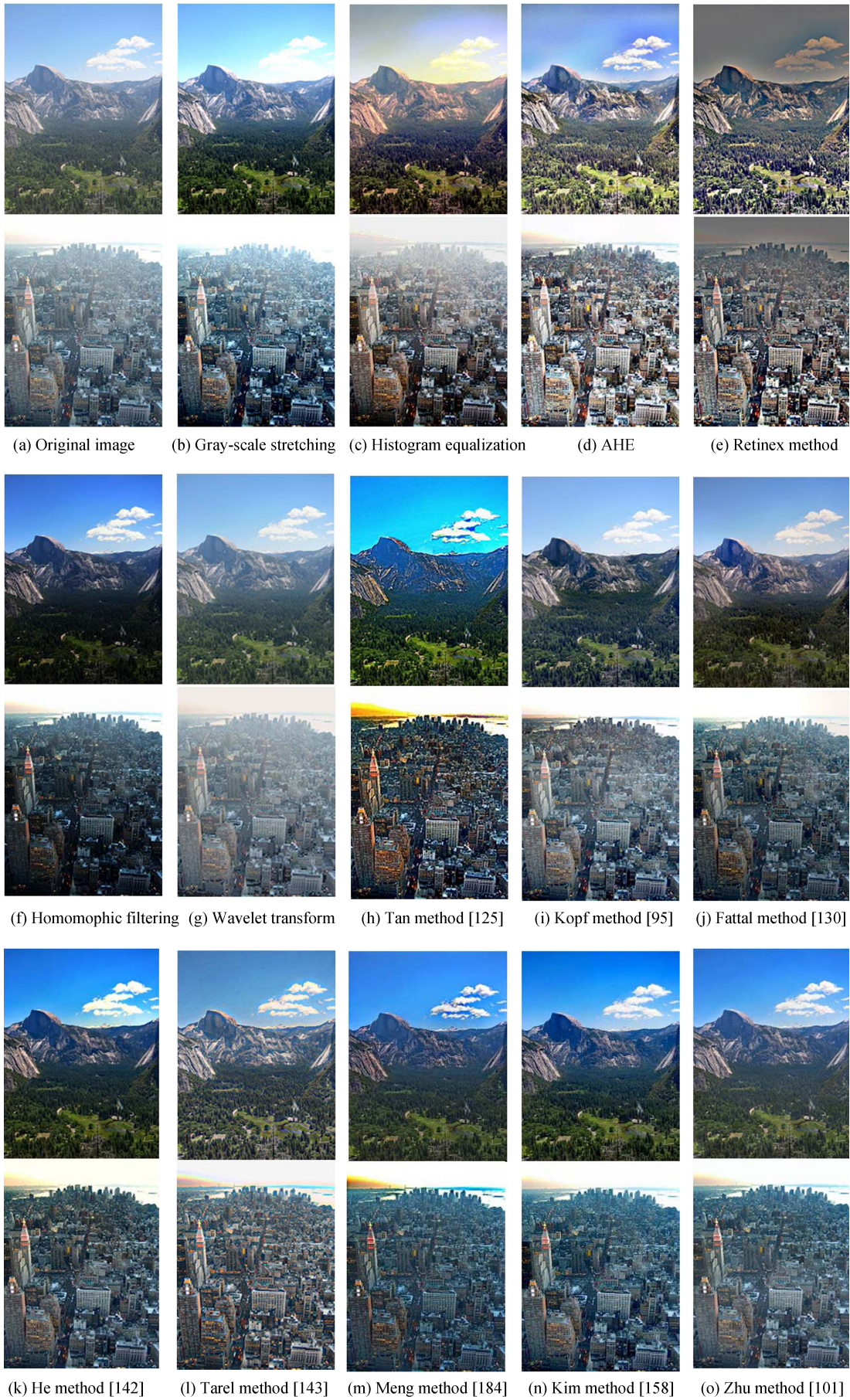


Fig. 20. Comparison of experimental results with various methods.

TABLE II  
OBJECTIVE EVALUATION OF VARIOUS METHODS ON “MOUNTAIN” IMAGE

Methods	PSNR	SSIM	$e$	$\bar{r}$	STD	AG	IE	NIQE	BIQI	BRISQE
Gray stretching	0.53	0.81	0.72	0.34	1.00	0.38	0.82	0.14	0.43	0.20
Histogram equalization	0.58	0.77	0.72	0.37	0.88	0.41	1.00	0.59	0.48	0.40
AHE	0.36	0.28	0.92	0.90	0.28	0.84	0.68	0.90	0.80	0.68
Retinex method	0	0	0.66	1.00	0.10	1.00	0.14	0	1.00	0.58
Homomorphic filtering	0.04	0.09	0.89	0.03	0.55	0.14	0.38	0.25	0	0
Wavelet transform	1.00	1.00	0	0	0.29	0	0.47	0.6	0.13	1.00
Tan method [125]	0.15	0.19	0.85	0.64	0.43	0.73	0.46	1.00	0.72	0.74
Kopf method [95]	0.42	0.81	0.81	0.39	0.70	0.38	0.60	0.08	0.43	0.19
Fattal method [130]	0.35	0.82	0.79	0.22	0.50	0.25	0.62	0.12	0.20	0.13
He method [142]	0.10	0.52	0.89	0.26	0.32	0.33	0.37	0.58	0.27	0.31
Tarel method [143]	0.37	0.67	1.00	0.54	0.12	0.53	0.50	1.00	0.49	0.58
Meng method [184]	0.13	0.69	0.94	0.27	0	0.35	0	0.41	0.31	0.38
Kim method [158]	0.13	0.57	0.77	0.40	0.27	0.44	0.57	0.50	0.43	0.43
Zhu method [101]	0.30	0.98	0.81	0.18	0.02	0.25	0.20	0.17	0.19	0.15

TABLE III  
OBJECTIVE EVALUATION OF VARIOUS METHODS ON “NEW YORK” IMAGE

Methods	PSNR	SSIM	$e$	$\bar{r}$	STD	AG	IE	NIQE	BIQI	BRISQE
Gray stretching	0.73	0.83	0.75	0.41	0.99	0.53	0.49	1.00	0.60	0.27
Histogram equalization	0.74	0.86	0.81	0.41	0.78	0.50	0.79	0.57	0.57	0.10
AHE	0.33	0.32	0.86	1.00	0.73	1.00	1.00	0.87	1.00	0.30
Retinex method	0	0.31	0.69	0.75	0.12	0.92	0.85	0.52	0.96	0.28
Homomorphic filtering	0.10	0.21	0.90	0.11	0.97	0.26	0.13	0.65	0.18	0.02
Wavelet transform	1.00	0.75	0	0	0	0	0.16	0	0	1.00
Tan method [125]	0.07	0	0.62	0.83	1.00	0.96	0.38	0.77	1.00	0.26
Kopf method [95]	0.58	0.96	0.82	0.42	0.53	0.48	0.49	0.80	0.48	0.06
Fattal method [130]	0.38	0.84	0.67	0.35	0.75	0.41	0.57	0.71	0.41	0.07
He method [142]	0.27	0.78	0.84	0.41	0.71	0.50	0.16	0.71	0.50	0.10
Tarel method [143]	0.46	0.73	1.00	0.60	0.53	0.65	0.63	0.67	0.67	0
Meng method [184]	0.23	0.69	0.90	0.42	0.63	0.50	0	0.73	0.50	0.11
Kim method [158]	0.35	0.77	0.75	0.50	0.73	0.57	0.42	0.76	0.59	0.15
Zhu method [101]	0.45	1.00	0.89	0.30	0.44	0.38	0.03	0.57	0.35	0.05

Among all of the methods, the Tan method [125], the He method [142] and the Tarel method [193] have the best dehazing effect on the whole hazy image, especially for long-range scenery. However, the Tan and Tarel methods resulted in color shifting or over saturation, which looks like pseudo color in the haze-free image. The Kopf method and the Fattal method can better maintain the color of the original image, but their overall effect lacks competitiveness. The Meng method [184], the Kim method [158] and the Zhu method [101] have similar results with relatively consistent tones. However, these three methods are not good at processing sharp-jumps in depth of field due to edges in the scene. Of the above image restoration methods, the He method [142] can achieve a good compromise of both close-up scenery and long-range scenery, while maintaining an outstanding visual effect on fidelity.

From the analysis of Fig. 20, it can be seen that overall, the image restoration methods are better than the image enhancement methods, especially in terms of color fidelity from a human visual perspective.

The objective IQA experiment is also implemented on the above images. Several IQA methods were selected including STD, AG, IE, PSNR, SSIM [222], Visible edges ( $e$ ,  $\bar{r}$ ) [223], BIQI [216], BRISQUE [217] and NIQE [218]. Since the IQA outputs have different dimensions, all data needs to be normalized. The formula is expressed as

$$y = \frac{(y_{\max} - y_{\min}) \times (x - x_{\min})}{x_{\max} - x_{\min}} + y_{\min} \quad (53)$$

where  $x_{\max}$  and  $x_{\min}$  are the maximum and minimum values of the data before normalization and  $y_{\max}$  and  $y_{\min}$  are the maximum and minimum values of the normalized data, respectively. In this paper,  $y_{\max} = 1$  and  $y_{\min} = 0$ , and each index's score is proportional to its performance. The experimental results for the images “Mountain” and “New York” are shown in Table II and Table III, respectively.

From Tables II and III, it can be easily seen that for the same method, different IQA indexes will give different scores. In some cases, the evaluation results have opposite values, since

the general IQA indexes are considering different aspects when evaluating a restored image. On the whole, the scores for the image restoration based methods are lower than the image enhancement based methods, especially for the histogram equalization and AHE which obtain very high scores, which conflicts with the subjective evaluation. This is mainly because this IQA focuses on the contrast and structure while ignoring the color fidelity. Combining the subjective evaluation of human vision, the above IQA indexes are not consistent with the subjective evaluation, and may not be suitable for direct evaluation of dehazed images. Thus, development of an IQA method for dehazed images is necessary for future work.

#### IV. CONCLUSIONS AND EXPECTATION

There are three types of dehazing methods seen in current research: image enhancement based methods, image fusion based methods and image restoration based methods. All of these methods have advantages and disadvantages. Image enhancement based methods improve the image contrast from the perspective of subjective vision, using a color correction which conforms to the perception of human visual system on a color scene. The early methods are mature and reliable, but these methods result in unpredictable distortion, especially where there is complex depth in the field image. Image fusion based methods maximize the beneficial information from multiple sources to finally form a high quality image. These methods do not need a physical model, but the fusion strategy for multiple sources of information is complex. Image restoration based methods are related to the image degradation mechanism, and are suitable for image dehazing with different depth of fields. However, optimal tools are required to find the solution and these methods may be time-consuming. In summary, image restoration based methods are better than the other two types of methods for real scene dehazing and is now the current research hotspot. The characteristics of some main approaches are shown in Table IV.

In view of the above analysis, some open questions that require further study are as follows.

1) Study of a comprehensive degradation model. The construction and resolution technique is core to physical model based methods for hazy image. At present, in addition to the widely-used atmospheric scattering model, there are other degradation models such as the dual-color atmospheric scattering model and the ATF (atmospheric transfer function) model. However, none of these models can accurately describe the phenomenon of haze degradation. Therefore, it is necessary to explore some cues that have been obtained from research results of modern atmospheric optics. In addition to considering the haze attenuation, another approach that should be explored is to introduce complex atmospheric light, atmospheric turbulence and other factors causing degradation of the image, so as to establish a more comprehensive physical model.

2) Explore the prior knowledge of the physical model. A reasonable priori is a prerequisite for success of single image dehazing methods based on physical models. Therefore, in order to accurately obtain the scene albedo, a clear scene prior is needed as well as a haze degradation prior for the

resolution of the model. For a clear image priori, it is necessary to consider the human visual color constancy, brightness constancy and contrast sensitivity as the research objects based on existing statistical priori, and exploit priori knowledge suitable for the human eye from clear images. From prior research on hazy image degradation, it is necessary to consider the feature variations with environmental light by combining the effect of turbid media and focusing on different types of scenarios, including different depths, different concentrations of haze, different light intensities and different backgrounds to explore universal priori knowledge, which can constrain the image solution process effectively and help to estimate the scene albedo precisely.

3) Integrate the image fusion approach and the image enhancement approach into the physical model. Many image enhancement methods have been developed based on the human vision system, which can quickly and accurately estimate the image brightness and maintain the true color. Image fusion methods can determine or mine effective information from different source images. Therefore, in physical model based dehazing methods, it is necessary to apply the human visual perception mechanism to the process of model resolution, and explore a fast and optimized method that uses multi scale information fusion technology and machine learning technology.

4) Strengthen research on video dehazing. Currently, most video dehazing methods are improvements of single image dehazing methods and usually contain a large number of complex data processing algorithms, such as large-scale matrix decomposition and mass equation group solutions. These complex operations often require a long processing time, but real-time performance of the algorithm is very important for certain application including safety monitoring systems and military reconnaissance systems. So it is important to establish how to effectively use potential information between adjacent frames in a video stream. In addition, use of programmable hardware to accelerate image dehazing is another future research direction.

5) Design a special IQA mechanism. Effective performance evaluation of image dehazing can guide the study of dehazing methods, and can lay the foundation for the design of closed-loop dehazing systems. At present, the research on quality assessment of dehazed images still requires further development, and the evaluation indexes are mainly concentrated on image clarity, contrast, color and structural information, while lacking comprehensive scientific criteria. The no-reference IQA method based on feature cognition can better fit human visual characteristics, which can be combined with an image analysis model, a statistical model, a visual information model and machine learning theory to evaluate the image dehazing objectively, and will be a very important research direction.

In summary, image dehazing techniques started relatively late due to the random nature and complexity of weather conditions, and there is only approximately a decade of research. At present, as a research hotspot in the field of machine vision, image dehazing techniques are developing rapidly, and a large number of new methods continue to appear. Although some

TABLE IV  
COMPARISON OF DIFFERENT APPROACHES

Category	Subclass	Methods	Characteristics
Image enhancement based method	Histogram equalization	Global histogram equalization	It is simple with high efficiency, suitable for overall enhancement of dark or bright images, but difficult for each local area to restore the optimal value.
		Local histogram equalization	It is suitable for processing of hazy images with changeable depth of field, but local block effects exist and there is a large calculation complexity.
	Retinex method	Single-scale Retinex	It is easy to implement, but difficult to keep a good balance between dynamic range compression and color constancy.
		Multi-scale Retinex	It can overcome the shortage of SSR but it does not have an edge preservation ability and will lead to halo phenomena.
	Frequency domain transform	Homomorphic filtering	It is suitable for the processing of images with uneven light, but its computation is large.
		Wavelet transform	It has the advantages of multi-scale analysis and multi-resolution characteristics on image contrast enhancement, but over-brightness, over-darkness and uneven illumination are difficult to resolve.
		Curvelet transform	It can improve the visual image quality by enhancing the curve edges but cannot remove the interference of fog in essence.
Image fusion based method	Fusion with multi-spectral image		This method does not need atmospheric light or a depth map, but it is difficult to obtain the source images and yield few halo artifacts.
	Fusion with single image		The images for fusion are to be perfectly aligned, but this technique is limited to processing color images.
Image restoration based method	Single image dehazing with additional information	Known the scene information	The restoration effect of the image is good, but scene information is needed from the sensors, or an existing database.
		User interaction	It can improve the visual effect and obvious contrast and it can run automatically in a real-time system.
		Machine learning	It runs fast and can achieve good results, but the training procedure is complex and the parameters rely on the training data.
	Multi-images dehazing with different conditions	Different polarizing conditions	It can enhance the contrast of the image in thin fog, but it is complicated to obtain the source images.
		Different weather conditions	It is simple and can achieve good results, but it is difficult to obtain the source images and it cannot be used in real-time systems.
	Single image dehazing with prior knowledge	Tan method [125]	It can maximize the local contrast with only one image, but easily results in color oversaturation in images with heavy haze.
		Fattal method [130]	It can usually produce impressive results when there is sufficient color information while it may fail in the cases where the original assumption is invalid.
		Kratz method [132]	It can recover a haze-free image with fine edge details, but the results often tend to be over enhanced and suffer from oversaturation.
	Tarel method [143]	He method [142]	It is simple and can keep high fidelity of the natural scene, but it is invalid when there are white objects.
		Kim method [158]	It simplifies the dehazing process and improves the efficiency, but many parameters in the algorithm cannot be adjusted adaptively.
			It can keep the balance between contrast enhancement and information loss, but it is not suitable for image dehazing with thick fog.

research works have shown outstanding results under certain conditions, these methods still need further improvement. Exploiting image dehazing methods with universality, robustness and real-time performance will be a challenging task in the future.

## REFERENCES

- [1] H. Halmaoui, A. Cord, and N. Hautiere, "Contrast restoration of road images taken in foggy weather," in *Proc. 2011 IEEE Int. Conf. Computer Vision Workshops*, Barcelona, Spain, 2011, pp. 2057–2063.
- [2] S. Bronte, L. M. Bergasa, and P. F. Alcantarilla, "Fog detection system based on computer vision techniques," in *Proc. 12th Int. IEEE Conf. Intelligent Transportation Systems*, St. Louis, MO, USA, 2009, pp. 1–6.
- [3] M. S. Shehata, J. Cai, W. M. Badawy, T. W. Burr, M. S. Pervez, R. J. Johannesson, and A. Radmanesh, "Video-based automatic incident detection for smart roads: The outdoor environmental challenges regarding false alarms," *IEEE Trans. Intell. Transp. Syst.*, vol. 9, no. 2, pp. 349–360, Jun. 2008.
- [4] S. C. Huang, B. H. Chen, and Y. J. Cheng, "An efficient visibility enhancement algorithm for road scenes captured by intelligent transportation systems," *IEEE Trans. Intell. Transp. Syst.*, vol. 15, no. 5, pp. 2321–2332, Oct. 2014.
- [5] S. C. Huang, "An advanced motion detection algorithm with video quality analysis for video surveillance systems," *IEEE Trans. Circuits Syst. Video Technol.*, vol. 21, no. 1, pp. 1–14, Jan. 2011.
- [6] B. Xie, F. Guo, and Z. X. Cai, "Universal strategy for surveillance video defogging," *Opt. Eng.*, vol. 51, no. 10, pp. 101703, May 2012.
- [7] Z. Jia, H. C. Wang, R. E. Caballero, Z. Y. Xiong, J. W. Zhao, and A. Finn, "A two-step approach to see-through bad weather for surveillance video quality enhancement," *Mach. Vis. Appl.*, vol. 23, no. 6, pp. 1059–1082, Nov. 2012.
- [8] I. Yoon, S. Kim, D. Kim, M. H. Hayes, and J. Paik, "Adaptive defogging with color correction in the HSV color space for consumer surveillance system," *IEEE Trans. Consum. Electron.*, vol. 58, no. 1, pp. 111–116, Feb. 2012.
- [9] K. B. Gibson, D. T. Vo, and T. Q. Nguyen, "An investigation of dehazing effects on image and video coding," *IEEE Trans. Image Proc.*, vol. 21, no. 2, pp. 662–673, Feb. 2012.
- [10] M. Chacon-Murguia and S. Gonzalez-Duarte, "An adaptive neural-fuzzy approach for object detection in dynamic backgrounds for surveillance systems," *IEEE Trans. on Industr. Electron.*, vol. 59, no. 8, pp. 3286–3298, Aug. 2012.
- [11] S. Y. Tao, H. J. Feng, Z. H. Xu, and Q. Li, "Image degradation and recovery based on multiple scattering in remote sensing and bad weather condition," *Opt. Express*, vol. 20, no. 15, pp. 16584–16595, Jul. 2012.
- [12] J. Long, Z. W. Shi, W. Tang, and C. S. Zhang, "Single remote sensing image dehazing," *IEEE Geosci. Remote Sens. Lett.*, vol. 11, no. 1, pp. 59–63, Jan. 2014.
- [13] A. Makarau, R. Richter, R. Muller, and P. Reinartz, "Haze detection and removal in remotely sensed multispectral imagery," *IEEE Trans. Geosci. Remote Sens.*, vol. 52, no. 9, pp. 5895–5905, Sep. 2014.
- [14] J. Liu, X. Wang, M. Chen, S. G. Liu, X. R. Zhou, Z. F. Shao, and P. Liu, "Thin cloud removal from single satellite images," *Opt. Express*, vol. 22, no. 1, pp. 618–632, Jan. 2014.
- [15] H. F. Li, L. P. Zhang, and H. F. Shen, "A principal component based haze masking method for visible images," *IEEE Geosci. Remote Sens. Lett.*, vol. 11, no. 5, pp. 975–979, May 2014.
- [16] X. X. Pan, F. Y. Xie, Z. G. Jiang, and J. H. Yin, "Haze removal for a single remote sensing image based on deformed haze imaging model," *IEEE Signal Process. Lett.*, vol. 22, no. 10, pp. 1806–1810, Oct. 2015.
- [17] L. X. Wang, W. X. Xie, and J. H. Pei, "Patch-based dark channel prior dehazing for RS multi-spectral image," *Chin. J. Electron.*, vol. 24, no. 3, pp. 573–578, Jul. 2015.
- [18] J. C. McCall and M. M. Trivedi, "Video-based lane estimation and tracking for driver assistance: Survey, system, and evaluation," *IEEE Trans. Intell. Transp. Syst.*, vol. 7, no. 1, pp. 20–37, Mar. 2006.
- [19] J. P. Tarel, N. Hautière, L. Caraffa, A. Cord, H. Halmaoui, and D. Gruyer, "Vision enhancement in homogeneous and heterogeneous fog," *IEEE Intell. Transp. Syst. Mag.*, vol. 4, no. 2, pp. 6–20, Apr. 2012.
- [20] M. Negru, S. Nedevschi, and R. I. Peter, "Exponential contrast restoration in fog conditions for driving assistance," *IEEE Trans. Intell. Transp. Syst.*, vol. 16, no. 4, pp. 2257–2268, Aug. 2015.
- [21] M. Pavlic, G. Rigoll, and S. Ilic, "Classification of images in fog and fog-free scenes for use in vehicles," in *Proc. 2013 IEEE Intelligent Vehicles Symposium*, 2013, pp. 481–486.
- [22] N. Hautière, J. P. Tarel, H. Halmaoui, R. Bremond, and D. Aubert, "Enhanced fog detection and free-space segmentation for car navigation," *Mach. Vis. Appl.*, vol. 25, no. 3, pp. 667–679, Apr. 2014.
- [23] N. Hautière, J. P. Tarel, and D. Aubert, "Mitigation of visibility loss for advanced camera-based driver assistance," *IEEE Trans. Intell. Transp. Syst.*, vol. 11, no. 2, pp. 474–484, Jun. 2010.
- [24] N. Hautière, J. P. Tarel, and D. Aubert, "Towards fog-free in-vehicle vision systems through contrast restoration," in *Proc. 2007 IEEE Conf. Computer Vision and Pattern Recognition*, Minneapolis, MN, USA, 2007, pp. 1–8.
- [25] H. J. Song, Y. Z. Chen, and Y. Y. Gao, "Velocity calculation by automatic camera calibration based on homogenous fog weather condition," *Int. J. Autom. Comput.*, vol. 10, no. 2, pp. 143–156, Apr. 2013.
- [26] R. Spinneker, C. Koch, S. B. Park, and J. J. Yoon, "Fast fog detection for camera based advanced driver assistance systems," in *Proc. IEEE 17th Int. Conf. Intelligent Transportation Systems*, Qingdao, China, 2014, pp. 1369–1374.
- [27] R. Sato, K. Domany, D. Deguchi, Y. Mekada, I. Ide, H. Murase, and Y. Tamatsu, "Visibility estimation of traffic signals under rainy weather conditions for smart driving support," in *Proc. 15th Int. IEEE Conf. Intelligent Transportation Systems*, Anchorage, AK, USA, 2012, pp. 1321–1326.
- [28] N. Carlevaris-Bianco, A. Mohan, and R. M. Eustice, "Initial results in underwater single image dehazing," in *Proc. 2010 IEEE OCEANS*, Seattle, WA, USA, 2010, pp. 1–8.
- [29] C. Ancuti, C. O. Ancuti, T. Haber, and P. Bekaert, "Enhancing underwater images and videos by fusion," in *Proc. 2012 IEEE Conf. Computer Vision and Pattern Recognition*, Providence, RI, 2012, pp. 81–88.
- [30] J. Y. Chiang and Y. C. Chen, "Underwater image enhancement by wavelength compensation and dehazing," *IEEE Trans. Image Process.*, vol. 21, no. 4, pp. 1756–1769, Apr. 2012.
- [31] P. Drews, E. do Nascimento, F. Moraes, S. Botelho, and M. Campos, "Transmission estimation in underwater single images," in *Proc. 2013 IEEE Int. Conf. Computer Vision Workshops*, Sydney, NSW, Australia, 2013, pp. 825–830.
- [32] H. M. Lu, Y. J. Li, and S. Serikawa, "Underwater image enhancement using guided trigonometric bilateral filter and fast automatic color correction," in *Proc. 20th IEEE Int. Conf. Image Processing*, Melbourne, VIC, Australia, 2013, pp. 3412–3416.
- [33] X. Y. Fu, P. X. Zhuang, Y. Huang, Y. H. Liao, X. P. Zhang, and X. H. Ding, "A retinex-based enhancing approach for single underwater image," in *Proc. 2014 IEEE Int. Conf. Image Processing*, Paris, France, 2014, pp. 4572–4576.
- [34] S. H. Sun, S. P. Fan, and Y. C. F. Wang, "Exploiting image structural similarity for single image rain removal," in *Proc. 2014 IEEE Int. Conf. Image Processing*, Paris, France, 2014, pp. 4482–4486.
- [35] S. D. You, R. T. Tan, R. Kawakami, and K. Ikeuchi, "Adherent raindrop detection and removal in video," in *Proc. 2013 IEEE Conf. Computer Vision and Pattern Recognition*, Portland, OR, USA, 2013, pp. 1035–1042.
- [36] M. Desvignes and G. Molinie, "Raindrops size from video and image processing," in *Proc. 19th IEEE Int. Conf. Image Processing*, Orlando, FL, USA, 2012, pp. 1341–1344.

- [37] Z. Jia, H. C. Wang, R. Caballero, Z. Y. Xiong, J. W. Zhao, and A. Finn, "Real-time content adaptive contrast enhancement for see-through fog and rain," in *Proc. 2010 IEEE Int. Conf. Acoustics Speech and Signal Processing*, Dallas, TX, USA, 2010, pp. 1378–1381.
- [38] K. Garg and S. K. Nayar, "When does a camera see rain?" in *Proc. 10th IEEE Int. Conf. Computer Vision*, Beijing, China, vol. 2, pp. 1067–1074, 2005.
- [39] H. Kawarabuki and K. Onoguchi, "Snowfall detection in a foggy scene," in *Proc. 22nd IEEE Int. Conf. Pattern Recognition*, Stockholm, Sweden, 2014, pp. 877–882.
- [40] L. R. Bissonnette, "Imaging through fog and rain," *Opt. Eng.*, vol. 31, no. 5, pp. 1045–1052, May 1992.
- [41] C. T. Cai, Q. Y. Zhang, and Y. H. Liang, "A survey of image dehazing approaches," in *Proc. 27th Chinese Control and Decision Conf.*, Qingdao, China, 2015, pp. 3964–3969.
- [42] Q. Wang and R. K. Ward, "Fast image/video contrast enhancement based on weighted thresholded histogram equalization," *IEEE Trans. Consum. Electron.*, vol. 53, no. 2, pp. 757–764, May 2007.
- [43] R. Dale-Jones and T. Tjahjadi, "A study and modification of the local histogram equalization algorithm," *Pattern Recogn.*, vol. 26, no. 9, pp. 1373–1381, Sep. 1993.
- [44] M. F. Khan, E. Khan, and Z. A. Abbasi, "Segment dependent dynamic multi-histogram equalization for image contrast enhancement," *Digit. Signal Process.*, vol. 25, pp. 198–223, Feb. 2014.
- [45] T. Celik and T. Tjahjadi, "Contextual and variational contrast enhancement," *IEEE Trans. Image Process.*, vol. 20, no. 12, pp. 3431–3441, Dec. 2011.
- [46] T. K. Kim, J. K. Paik, and B. S. Kang, "Contrast enhancement system using spatially adaptive histogram equalization with temporal filtering," *IEEE Trans. Consum. Electron.*, vol. 44, no. 1, pp. 82–87, Feb. 1998.
- [47] J. Y. Kim, L. S. Kim, and S. H. Hwang, "An advanced contrast enhancement using partially overlapped sub-block histogram equalization," *IEEE Trans. Circuits Syst. Video Technol.*, vol. 11, no. 4, pp. 475–484, Apr. 2001.
- [48] S. C. Huang and C. H. Yeh, "Image contrast enhancement for preserving mean brightness without losing image features," *Eng. Appl. Artif. Intell.*, vol. 26, no. 5–6, pp. 1487–1492, May–Jun. 2013.
- [49] H. T. Xu, G. T. Zhai, X. L. Wu, and X. K. Yang, "Generalized equalization model for image enhancement," *IEEE Trans. Multimed.*, vol. 16, no. 1, pp. 68–82, Jan. 2014.
- [50] L. J. Wang and R. Zhu, "Image defogging algorithm of single color image based on wavelet transform and histogram equalization," *Appl. Math. Sci.*, vol. 7, no. 79, pp. 3913–3921, 2013.
- [51] Z. Y. Xu, X. M. Liu, and N. Ji, "Fog removal from color images using contrast limited adaptive histogram equalization," in *Proc. 2nd IEEE Int. Congress on Image and Signal Processing*, Tianjin, China, 2009, pp. 1–5.
- [52] M. F. Al-Sammaraie, "Contrast enhancement of roads images with foggy scenes based on histogram equalization," in *Proc. 10th Int. Conf. Computer Science & Education*, Cambridge, UK, 2015, pp. 95–101.
- [53] G. Yadav, S. Maheshwari, and A. Agarwal, "Foggy image enhancement using contrast limited adaptive histogram equalization of digitally filtered image: Performance improvement," in *Proc. 2014 Int. Conf. Advances in Computing, Communications and Informatics*, New Delhi, India, 2014, pp. 2225–2231.
- [54] E. H. Land and J. J. McCann, "Lightness and Retinex theory," *J. Opt. Soc. Am.*, vol. 61, no. 1, pp. 1–11, Jan. 1971.
- [55] T. J. Cooper and F. A. Baqai, "Analysis and extensions of the Frankle-McCann retinex algorithm," *J. Electron. Image*, vol. 13, no. 1, pp. 85–92, Jan. 2004.
- [56] D. J. Jobson, Z. U. Rahman, and G. A. Woodell, "Properties and performance of a center/surround retinex," *IEEE Trans. Image Process.*, vol. 6, no. 3, pp. 451–462, Mar. 1997.
- [57] Z. U. Rahman, D. J. Jobson, and G. A. Woodell, "Multi-scale retinex for color image enhancement," in *Proc. IEEE Int. Conf. Image Processing*, Lausanne, Switzerland, vol. 3, pp. 1003–1006, 1996.
- [58] X. Xu, Q. Chen, P. A. Heng, H. J. Sun, and D. S. Xia, "A fast halo-free image enhancement method based on retinex," *J. Computer-Aided Des. Comput. Graph.*, vol. 20, no. 10, pp. 1325–1331, Oct. 2008.
- [59] W. T. Yang, R. G. Wang, S. Fang, and X. Zhang, "Variable filter retinex algorithm for foggy image enhancement," *J. Computer-Aided Des. Comput. Graph.*, vol. 22, no. 6, pp. 965–971, Jun. 2010.
- [60] W. W. Hu, R. G. Wang, S. Fang, and Q. Hu, "Retinex algorithm for image enhancement based on bilateral filtering," *J. Eng. Graph.*, vol. 31, no. 2, pp. 104–109, Apr. 2010.
- [61] X. Y. Hu, X. H. Gao, and H. B. Wang, "A novel retinex algorithm and its application to fog-degraded image enhancement," *Sens. Transd.*, vol. 175, no. 7, pp. 138–143, Jul. 2014.
- [62] T. Shu, Y. F. Liu, B. Deng, Y. P. Tan, and B. Q. Chen, "Multi-scale Retinex algorithm for the foggy image enhancement based on sub-band decomposition," *J. Jishou Univ.*, vol. 36, no. 1, pp. 40–45, Jan. 2015.
- [63] K. Zhang, C. C. Wu, J. X. Miao, and L. Z. Yi, "Research about using the retinex-based method to remove the fog from the road traffic video," *ICTIS 2013*, pp. 861–867.
- [64] M. J. Seow and V. K. Asari, "Ratio rule and homomorphic filter for enhancement of digital colour image," *Neurocomputing*, vol. 69, no. 7–9, pp. 954–958, Mar. 2006.
- [65] W. T. Cai, Y. X. Liu, M. C. Li, L. Cheng, and C. X. Zhang, "A self-adaptive homomorphic filter method for removing thin cloud," in *Proc. 19th Int. Conf. Geoinformatics*, Shanghai, China, 2011, pp. 1–4.
- [66] L. L. Grewe and R. B. Richard, "Atmospheric attenuation reduction through multi-sensor fusion," in *Proc. SPIE Sensor Fusion: Architectures, Algorithms and Applications II*, Orlando, FL, vol. 3376, pp. 102–109, 1998.
- [67] F. Russo, "An image enhancement technique combining sharpening and noise reduction," *IEEE Trans. Instrum. Meas.*, vol. 51, no. 4, pp. 824–828, Aug. 2002.
- [68] Y. Du, B. Guindon, and J. Cihlar, "Haze detection and removal in high resolution satellite image with wavelet analysis," *IEEE Trans. Geosci. Remote Sens.*, vol. 40, no. 1, pp. 210–217, Jan. 2002.
- [69] S. D. Zhou, M. Wang, F. Huang, Z. H. Liu, and S. Ye, "Color image defogging based on intensity wavelet transform and color improvement," *J. Harbin Univ. Sci. Technol.*, vol. 16, no. 4, pp. 59–62, Aug. 2011.
- [70] R. Zhu and L. J. Wang, "Improved wavelet transform algorithm for single image dehazing," *Optik-Int. J. Light Electron Opt.*, vol. 125, no. 13, pp. 3064–3066, Jul. 2014.
- [71] N. Anantrasirichai, A. Achim, D. Bull, and N. Kingsbury, "Mitigating the effects of atmospheric distortion using DT-CWT fusion," in *Proc. 19th IEEE Int. Conf. Image Processing*, Orlando, FL, USA, 2012, pp. 3033–3036.
- [72] J. John and M. Wilscy, "Enhancement of weather degraded color images and video sequences using wavelet fusion," in *Advances in Electrical Engineering and Computational Science*, S. L. Ao and L. Gelman, Eds. Netherlands: Springer, 2009, pp. 99–109.
- [73] J. L. Starck, F. Murtagh, E. J. Candes, and D. L. Donoho, "Gray and color image contrast enhancement by the curvelet transform," *IEEE Trans. Image Process.*, vol. 12, no. 6, pp. 706–717, Jun. 2003.
- [74] M. Verma, V. D. Kaushik, and V. K. Pathak, "An efficient deblurring algorithm on foggy images using curvelet transforms," in *Proc. 3rd Int. Symposium on Women in Computing and Informatics*, New York, NY, USA, 2015, pp. 426–431.
- [75] N. Salamat, A. Germain, and S. Süssstrunk, "Removing shadows from images using color and near-infrared," in *Proc. 18th IEEE Int. Conf. Image Processing*, Brussels, Belgium, 2011, pp. 1713–1716.
- [76] L. Schaul, C. Fredembach, and S. Süssstrunk, "Color image dehazing using the near-infrared," in *Proc. 16th IEEE Int. Conf. Image Processing*, Cairo, Egypt, 2009, pp. 1629–1632.
- [77] J. Son, H. Kwon, T. Shim, Y. Kim, S. Ahu, and K. Sohng, "Fusion method of visible and infrared images in foggy environment," in *Proc. Int. Conf. Image Processing, Computer Vision, and Pattern Recognition*, 2015, pp. 433–437.

- [78] C. Feng, S. J. Zhuo, X. P. Zhang, L. Shen, and S. Susstrunk, "Near-infrared guided color image dehazing," in *Proc. IEEE Int. Conf. Image Process.*, Melbourne, VIC, Australia, 2013, pp. 2363–2367.
- [79] C. O. Ancuti, C. Ancuti, and P. Bekaert, "Effective single image dehazing by fusion," in *Proc. 17th IEEE Int. Conf. Image Process.*, Hong Kong, China, 2010, pp. 3541–3544.
- [80] C. O. Ancuti and C. Ancuti, "Single image dehazing by multi-scale fusion," *IEEE Trans. Image Process.*, vol. 22, no. 8, pp. 3271–3282, Aug. 2013.
- [81] C. O. Ancuti, C. Ancuti, C. Hermans, and P. Bekaert, "Image and video decolorization by fusion," *Asian Conference on Computer Vision*, R. Kimmel, R. Klette, and A. Sugimoto, Eds. Berlin Heidelberg, Germany: Springer-Verlag, 2011, pp. 79–92.
- [82] S. Fang, R. Deng, Y. Cao, and C. L. Fang, "Effective single underwater image enhancement by fusion," *J. Comput.*, vol. 8, no. 4, pp. 904–911, Apr. 2013.
- [83] Z. L. Ma, J. Wen, C. Zhang, Q. Y. Liu, and D. N. Yan, "An effective fusion defogging approach for single sea fog image," *Neurocomputing*, vol. 173, pp. 1257–1267, Jan. 2016.
- [84] Z. Wang and Y. Feng, "Fast single haze image enhancement," *Comput. Electr. Eng.*, vol. 40, no. 3, pp. 785–795, Apr. 2014.
- [85] F. Guo, J. Tang, and Z. X. Cai, "Fusion strategy for single image dehazing," *Int. J. Digit. Content Technol. Appl.*, vol. 7, no. 1, pp. 19–28, Jan. 2013.
- [86] H. Zhang, X. Liu, Z. T. Huang, and Y. F. Ji, "Single image dehazing based on fast wavelet transform with weighted image fusion," in *Proc. 2014 IEEE Int. Conf. Image Processing*, Paris, France, 2014, pp. 4542–4546.
- [87] J. P. Oakley and B. L. Satherley, "Improving image quality in poor visibility conditions using a physical model for contrast degradation," *IEEE Trans. Image Process.*, vol. 7, no. 2, pp. 167–179, Feb. 1998.
- [88] E. J. McCartney, *Optics of the Atmosphere: Scattering by Molecules and Particles*. New York, USA: John Wiley and Sons, Inc., 1976, pp. 1–42.
- [89] K. Tan and J. P. Oakley, "Physics-based approach to color image enhancement in poor visibility conditions," *J. Opt. Soc. Am. A*, vol. 18, no. 10, pp. 2460–2467, 2001.
- [90] K. Tan and J. P. Oakley, "Enhancement of color images in poor visibility conditions," in *Proc. 2000 Int. Conf. Image Processing*, Vancouver, BC, Canada, 2000, pp. 788–791.
- [91] M. J. Robinson, D. W. Armitage, and J. P. Oakley, "Seeing in the mist: Real time video enhancement," *Sens. Rev.*, vol. 22, no. 2, pp. 157–161, Jun. 2002.
- [92] N. Hautière, J. P. Tarel, J. Lavenant, and D. Aubert, "Automatic fog detection and estimation of visibility distance through use of an onboard camera," *Mach. Vis. Appl.*, vol. 17, no. 1, pp. 8–20, Apr. 2006.
- [93] N. Hautière and D. Aubert, "Contrast restoration of foggy images through use of an onboard camera," in *Proc. 2005 IEEE Intelligent Transportation Systems*, Vienna, Austria, 2005, pp. 601–606.
- [94] N. Hautière, R. Labayrade, and D. Aubert, "Real-time disparity contrast combination for onboard estimation of the visibility distance," *IEEE Trans. Intell. Transp. Syst.*, vol. 7, no. 2, pp. 201–212, Jun. 2006.
- [95] J. Kopf, B. Neubert, B. Chen, M. F. Cohen, D. Cohen-Or, O. Deussen, M. Uyttendaele, and D. Lischinski, "Deep photo: Model-based photograph enhancement and viewing," *ACM Trans. Graphics (TOG)*, vol. 27, no. 5, Article ID 116, 2008.
- [96] S. G. Narasimhan and S. K. Nayar, "Interactive (de) weathering of an image using physical models," in *Proc. IEEE Workshop on Color and Photometric Methods in Computer Vision*, pp. 1–8, 2003.
- [97] Y. B. Sun, L. Xiao, Z. H. Wei, and H. Z. Wu, "Method of defogging image of outdoor scenes based on PDE," *J. Syst. Simul.*, vol. 19, no. 16, pp. 3739–3744, Aug. 2007.
- [98] K. T. Tang, J. C. Yang, and J. Wang, "Investigating haze-relevant features in a learning framework for image dehazing," in *Proc. 2014 IEEE Conf. Computer Vision and Pattern Recognition*, Columbus, OH, Italy, 2014, pp. 2995–3002.
- [99] K. B. Gibson, S. J. Belongie, and T. Q. Nguyen, "Example based depth from fog," in *Proc. 20th IEEE Int. Conf. Image Processing*, Melbourne, VIC, Australia, 2013, pp. 728–732.
- [100] Q. S. Zhu, J. M. Mai, and L. Shao, "Single image dehazing using color attenuation prior," in *Proc. 25th British Machine Vision Conference*, 2014, pp. 1–10.
- [101] Q. S. Zhu, J. M. Mai, and L. Shao, "A fast single image haze removal algorithm using color attenuation prior," *IEEE Trans. Image Process.*, vol. 24, no. 11, pp. 3522–3533, Nov. 2015.
- [102] Y. Y. Schechner, S. G. Narasimhan, and S. K. Nayar, "Instant dehazing of images using polarization," in *Proc. 2001 IEEE Computer Society Conf. Computer Vision and Pattern Recognition*, Kauai, HI, USA, 2001, pp. 325–332.
- [103] Y. Y. Schechner, S. G. Narasimhan, and S. K. Nayar, "Polarization-based vision through haze," *Appl. Opt.*, vol. 42, no. 3, pp. 511–525, Feb. 2003.
- [104] S. Shwartz, E. Namer, and Y. Y. Schechner, "Blind haze separation," in *Proc. 2006 IEEE Computer Society Conf. Computer Vision and Pattern Recognition*, New York, NY, USA, vol. 2, pp. 1984–1991, 2006.
- [105] Y. Y. Schechner and Y. Averbuch, "Regularized image recovery in scattering media," *IEEE Trans. Pattern Anal. Mach. Intell.*, vol. 29, no. 9, pp. 1655–1660, Sep. 2007.
- [106] R. Kaftory, Y. Y. Schechner, and Y. Y. Zeevi, "Variational distance-dependent image restoration," in *Proc. 2007 IEEE Conf. Computer Vision and Pattern Recognition*, Minneapolis, MN, USA, 2007, pp. 1–8.
- [107] F. Liu, L. Cao, X. P. Shao, P. L. Han, and X. L. Bin, "Polarimetric dehazing utilizing spatial frequency segregation of images," *Appl. Opt.*, vol. 54, no. 27, pp. 8116–8122, Sep. 2015.
- [108] S. Fang, X. S. Xia, H. Xing, and C. W. Chen, "Image dehazing using polarization effects of objects and airlight," *Opt. Express*, vol. 22, no. 16, pp. 19523–19537, Aug. 2014.
- [109] E. Namer, S. Shwartz, and Y. Schechner, "Skyless polarimetric calibration and visibility enhancement," *Opt. Express*, vol. 17, no. 2, pp. 472–493, Jan. 2009.
- [110] T. Treibitz and Y. Y. Schechner, "Polarization: Beneficial for visibility enhancement?," in *Proc. 2009 IEEE Conf. Computer Vision and Pattern Recognition*, Media, Iran, 2009, pp. 525–532.
- [111] C. L. Li, W. J. Lu, S. Xue, Y. C. Shi, and X. N. Sun, "Quality assessment of polarization analysis images in foggy conditions," in *Proc. 2014 IEEE Int. Conf. Image Processing*, Paris, France, 2014, pp. 551–555.
- [112] D. Miyazaki, D. Akiyama, M. Baba, R. Furukawa, S. Hiura, and N. Asada, "Polarization-based dehazing using two reference objects," in *Proc. 2013 IEEE Int. Conf. Computer Vision Workshops*, Washington, DC, USA, 2013, pp. 852–859.
- [113] Y. Y. Schechner and N. Karpel, "Clear underwater vision," in *Proc. 2004 IEEE Computer Society Conf. Computer Vision and Pattern Recognition*, Washington, DC, USA, 2004, pp. 536–543.
- [114] Y. Y. Schechner and N. Karpel, "Recovery of underwater visibility and structure by polarization analysis," *IEEE J. Oceanic Eng.*, vol. 30, no. 3, pp. 570–587, Jul. 2005.
- [115] T. Treibitz and Y. Y. Schechner, "Active polarization descattering," *IEEE Trans. Pattern Anal. Mach. Intell.*, vol. 31, no. 3, pp. 385–399, Mar. 2009.
- [116] S. K. Nayar and S. G. Narasimhan, "Vision in bad weather," in *Proc. 7th IEEE Int. Conf. Computer Vision*, Kerkyra, Greece, 1999, pp. 820–827.
- [117] S. G. Narasimhan and S. K. Nayar, "Chromatic framework for vision in bad weather," in *Proc. 2000 IEEE Conf. Computer Vision and Pattern Recognition*, Hilton Head Island, SC, USA, 2000, pp. 598–605.
- [118] S. G. Narasimhan and S. K. Nayar, "Vision and the atmosphere," *Int. J. Comput. Vis.*, vol. 48, no. 3, pp. 233–254, Jul. 2002.
- [119] S. G. Narasimhan and S. K. Nayar, "Contrast restoration of weather degraded images," *IEEE Trans. Pattern Anal. Mach. Intell.*, vol. 25, no. 6, pp. 713–724, Jun. 2003.

- [120] S. G. Narasimhan and S. K. Nayar, "Removing weather effects from monochrome images," in *Proc. 2001 IEEE Computer Society Conf. Computer Vision and Pattern Recognition*, Kauai, HI, USA, 2001, pp. 186–193.
- [121] J. Sun, J. Y. Jia, C. K. Tang, and H. Y. Shum, "Poisson matting," *ACM Trans. Graph.*, vol. 23, no. 3, pp. 315–321, Aug. 2004.
- [122] G. Chen, T. Wang, and H. Q. Zhou, "A novel physics-based method for restoration of foggy day images," *J. Image Graph.*, vol. 13, no. 5, pp. 885–893, May 2008.
- [123] D. Wu and Q. H. Dai, "Data-driven visibility enhancement using multi-camera system," in *Proc. SPIE Enhanced and Synthetic Vision*, Orlando, Florida, USA, vol. 7689, Article ID 76890H, 2010.
- [124] D. Wu and Q. S. Zhu, "The latest research progress of image dehazing," *Acta Autom. Sin.*, vol. 41, no. 2, pp. 221–239, Feb. 2015.
- [125] R. T. Tan, "Visibility in bad weather from a single image," in *Proc. 2008 IEEE Conf. Computer Vision and Pattern Recognition*, Anchorage, AK, USA, 2008, pp. 1–8.
- [126] C. Ancuti and C. O. Ancuti, "Effective contrast-based dehazing for robust image matching," *IEEE Geosci. Remote Sens. Lett.*, vol. 11, no. 11, pp. 1871–1875, Nov. 2014.
- [127] M. Bertalmio, V. Caselles, E. Provenzi, and A. Rizzi, "Perceptual color correction through variational techniques," *IEEE Trans. Image Process.*, vol. 16, no. 4, pp. 1058–1072, Apr. 2007.
- [128] A. Galdran, J. Vazquez-Corral, D. Pardo, and M. Bertalmio, "Enhanced variational image dehazing," *SIAM J. Imaging Sci.*, vol. 8, no. 3, pp. 1519–154, Feb. 2015.
- [129] A. Galdran, J. Vazquez-Corral, D. Pardo, and M. Bertalmio, "A variational framework for single image dehazing," in *Proc. 2014 Springer European Conf. Computer Vision*, Zurich, Switzerland, 2014, pp. 259–270.
- [130] R. Fattal, "Single image dehazing," *ACM Trans. Graph. (TOG)*, vol. 27, no. 3, Article ID 72, Aug. 2008.
- [131] R. Fattal, "Dehazing using color-lines," *ACM Trans. Graph. (TOG)*, vol. 34, no. 1, Article ID 13, Nov. 2014.
- [132] L. Kratz and K. Nishino, "Factorizing scene albedo and depth from a single foggy image," in *Proc. IEEE 12th Int. Conf. Computer Vision*, Kyoto, Japan, 2009, pp. 1701–1708.
- [133] K. Nishino, L. Kratz, and S. Lombardi, "Bayesian defogging," *Int. J. Computer Vis.*, vol. 98, no. 3, pp. 263–278, Jul. 2012.
- [134] L. Caraffa and J. P. Tarel, "Stereo reconstruction and contrast restoration in daytime fog," in *Proc. 11th Asia Conf. Computer Vision*, Daejeon, Korea, 2013, pp. 13–25.
- [135] L. Caraffa and J. P. Tarel, "Markov random field model for single image defogging," in *Proc. 2013 IEEE Intelligent Vehicles Symposium*, Gold Coast, QLD, Australia, 2013, pp. 994–999.
- [136] D. Nan, D. Y. Bi, C. Liu, S. P. Ma, and L. Y. He, "A Bayesian framework for single image dehazing considering noise," *Sci. World J.*, Vol. 2014, Article ID 651986, 2014.
- [137] L. Mutimbu and A. Robles-Kelly, "A relaxed factorial Markov random field for colour and depth estimation from a single foggy image," in *Proc. 20th IEEE Int. Conf. Image Processing*, Melbourne, VIC, Australia, 2013, pp. 355–359.
- [138] X. M. Dong, X. Y. Hu, S. L. Peng, and D. C. Wang, "Single color image dehazing using sparse priors," in *Proc. 17th IEEE Int. Conf. Image Processing*, Hong Kong, China, 2010, pp. 3593–3596.
- [139] J. W. Zhang, L. Li, G. Q. Yang, Y. Zhang, and J. Z. Sun, "Local albedo-insensitive single image dehazing," *Vis. Comput.*, vol. 26, no. 6–8, pp. 761–768, Jun. 2010.
- [140] J. W. Zhang, L. Li, Y. Zhang, G. Q. Yang, X. C. Cao, and J. Z. Sun, "Video dehazing with spatial and temporal coherence," *Vis. Comput.*, vol. 27, no. 6–8, pp. 749–757, Jun. 2011.
- [141] Y. K. Wang and C. T. Fan, "Single image defogging by multiscale depth fusion," *IEEE Trans. Image Process.*, vol. 23, no. 11, pp. 4826–4837, Nov. 2014.
- [142] K. M. He, J. Sun, and X. O. Tang, "Single image haze removal using dark channel prior," in *Proc. IEEE Conf. Computer Vision and Pattern Recognition*, New York, USA, 2009, pp. 1956–1963.
- [143] K. M. He, J. Sun, and X. O. Tang, "Single image haze removal using dark channel prior," *IEEE Trans. Pattern Anal. Mach. Intell.*, vol. 33, no. 12, pp. 2341–2353, Dec. 2011.
- [144] A. Levin, D. Lischinski, and Y. Weiss, "A closed-form solution to natural image matting," *IEEE Trans. Pattern Anal. Mach. Intell.*, vol. 30, no. 2, pp. 228–242, Feb. 2008.
- [145] K. B. Gibson and T. Q. Nguyen, "On the effectiveness of the dark channel prior for single image dehazing by approximating with minimum volume ellipsoids," in *Proc. IEEE Int. Conf. Acoustics, Speech, and Single Processing*, Prague, Czech Republic, 2011, pp. 1253–1256.
- [146] K. B. Gibson and T. Q. Nguyen, "An analysis of single image defogging methods using a color ellipsoid framework," *EURASIP J. Image Video Process.*, vol. 2013, pp. 37, Jan. 2013.
- [147] D. Park, D. K. Han, and H. Ko, "Single image haze removal with WLS-based edge-preserving smoothing filter," in *Proc. 2013 IEEE Int. Conf. Acoustics, Speech and Signal Processing*, Vancouver, BC, Canada, 2013, pp. 2469–2473.
- [148] J. Yu, C. B. Xiao, and D. P. Li, "Physics-based fast single image fog removal," in *Proc. IEEE 10th Int. Conf. Signal Processing*, Beijing, China, 2010, pp. 1048–1052.
- [149] C. H. Yeh, L. W. Kang, M. S. Lee, and C. Y. Lin, "Haze effect removal from image via haze density estimation in optical model," *Opt. Express*, vol. 21, no. 22, pp. 27127–27141, Nov. 2013.
- [150] S. Fang, J. Q. Zhan, Y. Cao, and R. Z. Rao, "Improved single image dehazing using segmentation," in *Proc. 17th IEEE Int. Conf. Image Processing*, Hong Kong, China, 2010, pp. 3589–3592.
- [151] F. C. Cheng, C. H. Lin, and J. L. Lin, "Constant time O(1) image fog removal using lowest level channel," *Electron. Lett.*, vol. 48, no. 22, pp. 1404–1406, Oct. 2012.
- [152] L. Chen, B. L. Guo, J. Bi, and J. J. Zhu, "Algorithm of single image fog removal based on joint bilateral filter," *J. Beijing Univ. Posts Telecomm.*, vol. 35, no. 4, pp. 19–23, Aug. 2012.
- [153] S. Serikawa and H. M. Lu, "Underwater image dehazing using joint trilateral filter," *Comput. Electr. Eng.*, vol. 40, no. 1, pp. 41–50, Jan. 2014.
- [154] K. M. He, J. Sun, and X. O. Tang, "Guided image filtering," in *Proc. 11th European Conf. Computer Vision*, Berlin Heidelberg, Germany, 2010, pp. 1–14.
- [155] K. M. He, J. Sun, and X. O. Tang, "Guided image filtering," *IEEE Trans. Pattern Anal. Mach. Intell.*, vol. 35, no. 6, pp. 1397–1409, Jun. 2013.
- [156] R. J. Gao, X. Fan, J. L. Zhang, and Z. X. Luo, "Haze filtering with aerial perspective," in *Proc. 19th IEEE Int. Conf. Image Processing*, Orlando, FL, USA, 2012, pp. 989–992.
- [157] F. Guo, J. Tang, and Z. X. Cai, "Image dehazing based on haziness analysis," *Int. J. Com.*, vol. 11, no. 1, pp. 78–86, Feb. 2011.
- [158] J. H. Kim, W. D. Jang, J. Y. Sim, and C. S. Kim, "Optimized contrast enhancement for real-time image and video dehazing," *J. Vis. Communun. Image Represent.*, vol. 24, no. 3, pp. 410–425, Apr. 2013.
- [159] C. Feng, F. P. Da, and C. X. Wang, "Single image dehazing using dark channel prior and adjacent region similarity," in *Proc. Chinese Conf. Pattern Recognition*, Beijing, China, 2012, pp. 463–470.
- [160] Z. L. Ma, J. Wen, and L. L. Hao, "Video image defogging algorithm for surface ship scenes," *Syst. Eng. Electron.*, vol. 36, no. 9, pp. 1860–1867, 2014.
- [161] Z. G. Li, J. H. Zheng, Z. J. Zhu, W. Yao, and S. Q. Wu, "Weighted guided image filtering," *IEEE Trans. Image Process.*, vol. 24, no. 1, pp. 120–129, Jan. 2015.
- [162] Z. G. Li and J. H. Zheng, "Edge-preserving decomposition-based single image haze removal," *IEEE Trans. Image Process.*, vol. 24, no. 12, pp. 5432–5441, Dec. 2015.
- [163] Z. G. Li, J. H. Zheng, W. Yao, and Z. J. Zhu, "Single image haze removal via a simplified dark channel," in *Proc. 2015 IEEE Int.*

- Conf. Acoustics, Speech and Signal Processing*, South Brisbane, QLD, Australia, 2015, pp. 1608–1612.
- [164] J. B. Wang, N. He, L. L. Zhang, and K. Lu, “Single image dehazing with a physical model and dark channel prior,” *Neurocomputing*, vol. 149, pp. 718–728, Feb. 2015.
- [165] A. K. Tripathi and S. Mukhopadhyay, “Single image fog removal using anisotropic diffusion,” *IET Image Process.*, vol. 6, no. 7, pp. 966–975, Oct. 2012.
- [166] F. M. Fang, F. Li, and T. Y. Zeng, “Single image Dehazing and Denoising: A fast variational approach,” *SIAM J. Imaging Sci.*, vol. 7, no. 2, pp. 969–996, Apr. 2014.
- [167] B. Li, S. H. Wang, J. Zheng, and L. P. Zheng, “Single image haze removal using content-adaptive dark channel and post enhancement,” *IET Comput. Vis.*, vol. 8, no. 2, pp. 131–140, Apr. 2014.
- [168] Y. H. Shiau, H. Y. Yang, P. Y. Chen, and Y. Z. Chuang, “Hardware implementation of a fast and efficient haze removal method,” *IEEE Trans. Circuits Syst. Video Technol.*, vol. 23, no. 8, pp. 1369–1374, Aug. 2013.
- [169] W. Sun, B. L. Guo, D. J. Li, and W. Jia, “Fast single-image dehazing method for visible-light systems,” *Opt. Eng.*, vol. 52, no. 9, pp. 093103, May 2013.
- [170] M. Ding and R. F. Tong, “Efficient dark channel based image dehazing using quadtrees,” *Sci. China Inf. Sci.*, vol. 56, no. 9, pp. 1–9, Sep. 2013.
- [171] X. M. Zhu, Y. Li, and Y. Qiao, “Fast single image dehazing through edge-guided interpolated filter,” in *Proc. 14th IAPR Int. Conf. Machine Vision Applications*, Tokyo, Japan, 2015, pp. 443–446.
- [172] K. B. Gibson and T. Q. Nguyen, “Fast single image fog removal using the adaptive wiener filter,” in *Proc. 20th IEEE Int. Conf. Image Processing*, Melbourne, VI, Australia, 2013, pp. 714–718.
- [173] S. C. Huang, B. H. Chen, and W. J. Wang, “Visibility restoration of single hazy images captured in real-world weather conditions,” *IEEE Trans. Circuits Syst. Video Technol.*, vol. 24, no. 10, pp. 1814–1824, Oct. 2014.
- [174] S. C. Huang, J. H. Ye, and B. H. Chen, “An advanced single-image visibility restoration algorithm for real-world hazy scenes,” *IEEE Trans. Industr. Electron.*, vol. 62, no. 5, pp. 2962–2972, May 2015.
- [175] J. G. Wang, S. C. Tai, and C. J. Lin, “Image haze removal using a hybrid of fuzzy inference system and weighted estimation,” *J. Electron. Imaging*, vol. 24, no. 3, Article ID 033027, Jun. 2015.
- [176] W. Sun, “A new single-image fog removal algorithm based on physical model,” *Optik-Int. J. Light Electron Opt.*, vol. 124, no. 21, pp. 4770–4775, Nov. 2013.
- [177] W. Sun, H. Wang, C. H. Sun, B. L. Guo, W. Y. Jia, and M. G. Sun, “Fast single image haze removal via local atmospheric light veil estimation,” *Comput. Electr. Eng.*, vol. 46, pp. 371–383, Aug. 2015.
- [178] H. B. Liu, J. Yang, Z. P. Wu, and Q. N. Zhang, “Fast single image dehazing based on image fusion,” *J. Electron. Imaging*, vol. 24, Article ID 013020, Jan. 2015.
- [179] W. Wang, W. H. Li, Q. J. Guan, and M. Qi, “Multiscale single image dehazing based on adaptive wavelet fusion,” *Math. Probl. Eng.*, vol. 2015, Article ID 131082, May 2015.
- [180] Y. H. Shiau, P. Y. Chen, H. Y. Yang, C. H. Chen, and S. S. Wang, “Weighted haze removal method with halo prevention,” *J. Visual Commun. Image Represent.*, vol. 25, no. 2, pp. 445–453, Feb. 2014.
- [181] J. Chen and L. P. Chau, “An enhanced window-variant dark channel prior for depth estimation using single foggy image,” in *Proc. IEEE Int. Conf. Image Processing*, Melbourne, VIC, Australia, 2013, pp. 3508–3512.
- [182] T. H. Kil, S. H. Lee, and N. I. Cho, “Single image dehazing based on reliability map of dark channel prior,” in *Proc. 20th IEEE Int. Conf. Image Processing*, Melbourne, VIC, Australia, 2013, pp. 882–885.
- [183] D. Wang and J. Zhu, “Fast smoothing technique with edge preservation for single image dehazing,” *IET Comput. Vis.*, vol. 9, no. 6, pp. 950–959, Dec. 2015.
- [184] G. F. Meng, Y. Wang, J. Y. Duan, S. M. Xiang, and C. H. Pan, “Efficient image dehazing with boundary constraint and contextual regularization,” in *Proc. 2013 IEEE Int. Conf. Computer Vision*, Sydney, NSW, Australia, 2013, pp. 617–624.
- [185] B. H. Chen, S. C. Huang, and J. H. Ye, “Hazy image restoration by bi-histogram modification,” *ACM Trans. Intell. Syst. Technol.*, vol. 6, no. 4, Article ID 50, Jul. 2015.
- [186] B. H. Chen and S. C. Huang, “An advanced visibility restoration algorithm for single hazy images,” *ACM Trans. Multimed. Comput. Commun. Appl. (TOMM)*, vol. 11, no. 4, Article ID 53, Apr. 2015.
- [187] C. O. Ancuti, C. Ancuti, C. Hermans, and P. Bekaert, “A fast semi-inverse approach to detect and remove the haze from a single image,” in *Proc. 10th Asian Conf. Computer Vision*, Berlin, Heidelberg, Germany, 2010, pp. 501–514.
- [188] Y. Y. Gao, H. M. Hu, S. H. Wang, and B. Li, “A fast image dehazing algorithm based on negative correction,” *Signal Process.*, vol. 103, pp. 380–398, Oct. 2014.
- [189] J. F. Li, H. Zhang, D. Yuan, and H. L. Wang, “Haze removal from single images based on a luminance reference model,” in *Proc. 2nd Asian Conf. Pattern Recognition*, Naha, Japan, 2013, pp. 446–450.
- [190] S. C. Pei and T. Y. Lee, “Nighttime haze removal using color transfer pre-processing and dark channel prior,” in *Proc. 19th IEEE Int. Conf. Image Processing*, Orlando, FL, USA, 2012, pp. 957–960.
- [191] J. Zhang, Y. Cao, and Z. F. Wang, “Nighttime haze removal based on a new imaging model,” in *Proc. 2014 IEEE Int. Conf. Image Processing*, Paris, France, 2014, pp. 4557–4561.
- [192] X. S. Jiang, H. X. Yao, S. P. Zhang, X. S. Lu, and W. Zeng, “Night video enhancement using improved dark channel prior,” in *Proc. 20th IEEE Int. Conf. Image Processing*, Melbourne, VIC, Australian, 2013, pp. 553–557.
- [193] J. P. Tarel and N. Hautiere, “Fast visibility restoration from a single color or gray level image,” in *Proc. IEEE 12th Int. Conf. Computer Vision*, Kyoto, Japan, 2009, pp. 2201–2208.
- [194] K. B. Gibson and T. Q. Nguyen, “Hazy image modeling using color ellipsoids,” in *Proc. 18th IEEE Int. Conf. Image Processing*, Brussels, Belgium, 2011, pp. 1861–1864.
- [195] J. Yu and Q. M. Liao, “Fast single image fog removal using edge-preserving smoothing,” in *Proc. 2011 IEEE Int. Conf. Acoustics, Speech and Signal Processing*, Prague, Czech Republic, 2011, pp. 1245–1248.
- [196] C. Tomasi and R. Manduchi, “Bilateral filtering for gray and color images,” in *Proc. 6th IEEE Int. Conf. Computer Vision*, Bombay, India, 1998, pp. 839–846.
- [197] H. Y. Zhao, C. B. Xiao, J. Yu, and X. J. Xu, “Single image fog removal based on local extrema,” *IEEE/CAA J. Autom. Sin.*, vol. 2, no. 2, pp. 158–165, Apr. 2015.
- [198] C. X. Xiao and J. J. Gan, “Fast image dehazing using guided joint bilateral filter,” *Vis. Comput.*, vol. 28, no. 6–8, pp. 713–721, Jun. 2012.
- [199] J. Kopf, M. F. Cohen, D. Lischinski, and M. Uyttendaele, “Joint bilateral upsampling,” *ACM Trans. Graph.*, vol. 26, no. 3, Article ID 96, Jul. 2007.
- [200] L. C. Bao, Y. B. Song, Q. X. Yang, and N. Ahuja, “An edge-preserving filtering framework for visibility restoration,” in *Proc. 21st Int. Conf. Pattern Recognition*, Tsukuba, Japan, 2012, pp. 384–387.
- [201] Q. Yan, L. Xu, and J. Y. Jia, “Dense scattering layer removal,” in *Proc. ACM SIGGRAPH Asia 2013 Technical Briefs*, New York, NY, USA, 2013.
- [202] X. Liu, F. X. Zeng, Z. T. Huang, and Y. F. Ji, “Single color image dehazing based on digital total variation filter with color transfer,” in *Proc. 20th IEEE Int. Conf. Image Processing*, Melbourne, VIC, Australia, 2013, pp. 909–913.
- [203] M. Negru, S. Nedevschi, and R. I. Peter, “Exponential image enhancement in daytime fog conditions,” in *Proc. 17th IEEE Int. Conf. Intelligent Transportation Systems*, Qingdao, China, 2014, pp. 1675–1681.
- [204] J. F. Li, H. Zhang, D. Yuan, and M. G. Sun, “Single image dehazing using the change of detail prior,” *Neurocomputing*, vol. 156, pp. 1–11, May 2015.

- [205] J. H. Kim, J. Y. Sim, and C. S. Kim, "Single image dehazing based on contrast enhancement," in *Proc. 2011 IEEE Int. Conf. Acoustics, Speech and Signal Processing*, Prague, Czech Republic, 2011, pp. 1273–1276.
- [206] H. Park, D. Park, D. K. Han, and H. Ko, "Single image haze removal using novel estimation of atmospheric light and transmission," in *Proc. IEEE Int. Conf. Image Processing*, Paris, France, 2014, pp. 4502–4506.
- [207] H. Park, D. Park, D. K. Han, and H. Ko, "Single image dehazing with image entropy and information fidelity," in *Proc. 2014 IEEE Int. Conf. Image Processing*, Paris, France, 2014, pp. 4037–4041.
- [208] Y. S. Lai, Y. L. Chen, and C. T. Hsu, "Single image dehazing with optimal transmission map," in *Proc. 21st IEEE Int. Conf. Pattern Recognition*, Tsukuba, Japan, 2012, pp. 388–391.
- [209] Y. H. Lai, Y. L. Chen, C. J. Chiou, and C. T. Hsu, "Single-image dehazing via optimal transmission map under scene priors," *IEEE Trans. Circuits Syst. Video Technol.*, vol. 25, no. 1, pp. 1–14, Jan. 2015.
- [210] M. Pedone and J. Heikkilä, "Robust airlight estimation for haze removal from a single image," in *Proc. 2011 IEEE Computer Society Conf. Computer Vision and Pattern Recognition Workshops*, Colorado Springs, CO, USA, 2011, pp. 90–96.
- [211] F. C. Cheng, C. C. Cheng, P. H. Lin, and S. C. Huang, "A hierarchical airlight estimation method for image fog removal," *Eng. Appl. Artif. Intell.*, vol. 43, pp. 27–34, Aug. 2015.
- [212] T. O. Aydin, R. Mantiuk, K. Myszkowski, and H. S. Seidel, "Dynamic range independent image quality assessment," *ACM Trans. Graph. (TOG)*, vol. 27, no. 3, Article ID 69, Aug. 2008.
- [213] K. Q. Huang, Q. Wang, and Z. Y. Wu, "Natural color image enhancement and evaluation algorithm based on human visual system," *Comput. Vis. Image Underst.*, vol. 103, no. 1, pp. 52–63, Jul. 2006.
- [214] B. S. Manjunath, J. R. Ohm, V. V. Vasudevan, and A. Yamada, "Color and texture descriptors," *IEEE Trans. Circuits Syst. Video Technol.*, vol. 11, no. 6, pp. 703–715, Jun. 2001.
- [215] K. D. Ma, W. T. Liu, and Z. Wang, "Perceptual evaluation of single image dehazing algorithms," in *Proc. 2015 IEEE Int. Conf. Image Processing*, Quebec City, QC, Canada, 2015, pp. 3600–3604.
- [216] A. K. Moorthy and A. C. Bovik, "A two-step framework for constructing blind image quality indices," *IEEE Signal Process. Lett.*, vol. 17, no. 5, pp. 513–516, May 2010.
- [217] A. Mittal, A. K. Moorthy, and A. C. Bovik, "No-reference image quality assessment in the spatial domain," *IEEE Trans. Image Process.*, vol. 21, no. 12, pp. 4695–4708, Dec. 2012.
- [218] A. Mittal, R. Soundararajan, and A. C. Bovik, "Making a completely blind image quality analyzer," *IEEE Signal Process. Lett.*, vol. 20, no. 3, pp. 209–212, Mar. 2013.
- [219] M. A. Saad, A. C. Bovik, and C. Charrier, "Blind image quality assessment: A natural scene statistics approach in the dct domain," *IEEE Trans. Image Process.*, vol. 21, no. 8, pp. 3339–3352, Aug. 2012.
- [220] Q. B. Wu, H. L. Li, K. N. Ngan, B. Zeng, and M. Gabbouj, "No reference image quality metric via distortion identification and multi-channel label transfer," in *Proc. 2014 IEEE Int. Symposium on Circuits and Systems*, Melbourne VIC, Australia, 2014, pp. 530–533.
- [221] Y. M. Fang, K. D. Ma, Z. Wang, W. S. Lin, Z. J. Fang, and G. T. Zhai, "No-reference quality assessment of contrast-distorted images based on natural scene statistics," *IEEE Signal Process. Lett.*, vol. 22, no. 7, pp. 838–842, Jul. 2015.
- [222] Z. Wang, A. C. Bovik, H. R. Sheikh, and E. P. Simoncelli, "Image quality assessment: From error visibility to structural similarity," *IEEE Trans. Image Process.*, vol. 13, no. 4, pp. 600–612, Apr. 2004.
- [223] N. Hautière, J. P. Tarel, D. Aubert, and E. Dumont, "Blind contrast enhancement assessment by gradient ratioing at visible edges," *Image Anal. Stereol. J.*, vol. 27, no. 2, pp. 87–95, Jun. 2008.
- [224] L. K. Choi, J. You, and A. C. Bovik, "Referenceless prediction of perceptual fog density and perceptual image defogging," *IEEE Trans. Image Process.*, vol. 24, no. 11, pp. 3888–3901, Nov. 2015.
- [225] D. P. Li, J. Yu, and C. B. Xiao, "No-reference quality assessment method for defogged images," *J. Image Graph.*, vol. 16, no. 9, pp. 1753–1757, Sep. 2011.
- [226] F. Guo and Z. X. Cai, "Objective assessment method for the clearness effect of image defogging algorithm," *Acta Autom. Sin.*, vol. 38, no. 9, pp. 1410–1419, Sep. 2012.
- [227] Z. Y. Chen, T. T. Jiang, and Y. H. Tian, "Quality assessment for comparing image enhancement algorithms," in *Proc. 2014 IEEE Conf. Computer Vision and Pattern Recognition*, Columbus, OH, Italy, 2014, pp. 3003–3010.



**Wencheng Wang** received the B.S. degree in automatic engineering in 2002, the M.S. and Ph.D. degrees in pattern recognition and intelligent system from Shandong University, Jinan, in 2005 and 2011, respectively. And now he is an associate professor of Department of Information and Control Engineering in Weifang University. From 2006 to 2007, he was a visiting scholar at Qingdao University of Science and Technology, and now he is a visiting scholar in University of North Texas and engaging in the research of computer vision and automatic detection on image dehazing. His group has published and authored more than 30 papers on academic journals and conference, four book chapters and 5 patents, and more than 30 papers have been indexed by SCI/EI. His main research interests include computer vision, pattern recognition, and intelligent computing. He is currently serving as an associate editor of international journal *Transactions of the Institute of Measurement and Control*. He was awarded the Young researchers award of Weifang University in 2010.



**Xiaohui Yuan** received the B.S. degree in electrical engineering from Hefei University of Technology, China in 1996 and Ph.D. degree in computer science from Tulane University in 2004. After his graduation, he worked at the National Institutes of Health on medical imaging and analysis till 2006. He joined the University of North Texas (UNT) as an Assistant Professor in 2006 and was promoted to Associate Professor with tenure in 2012. His research interests include computer vision, data mining, machine learning, and artificial intelligence. He served as PI and co-PI in projects supported by Air Force Laboratory, National Science Foundation (NSF), Texas Advanced Research Program, Oak Ridge Associated Universities, and UNT. His research findings are reported in over 70 peer-reviewed papers. Dr. Yuan is a recipient of Ralph E. Powe Junior Faculty Enhancement award in 2008 and the Air Force Summer Faculty Fellowship in 2011, 2012, and 2013. He also received two research awards and a teaching award from UNT in 2007, 2008, and 2012, respectively. He served in the editorial board of several international journals and served as session chairs in many conferences, as well as panel reviewer for funding agencies including NSF, NIH, and Louisiana Board of Regents Research Competitiveness program. He is a member of IEEE and SPIE.